Unraveling the Intricate Organization of Mammalian Mitochondrial Presequence Translocases: Existence of Multiple Translocases for Maintenance of Mitochondrial Function

Devanjan Sinha, Shubhi Srivastava, Lekshmi Krishna, Patrick D'Silva

Department of Biochemistry, Indian Institute of Science, Bangalore, India

Mitochondria are indispensable organelles implicated in multiple aspects of cellular processes, including tumorigenesis. Heat shock proteins play a critical regulatory role in accurately delivering the nucleus-encoded proteins through membrane-bound presequence translocase (Tim23 complex) machinery. Although altered expression of mammalian presequence translocase components had been previously associated with malignant phenotypes, the overall organization of Tim23 complexes is still unsolved. In this report, we show the existence of three distinct Tim23 complexes, namely, B1, B2, and A, involved in the maintenance of normal mitochondrial function. Our data highlight the importance of Magmas as a regulator of translocase function and in dynamically recruiting the J-proteins DnaJC19 and DnaJC15 to individual translocases. The basic housekeeping function involves translocases B1 and B2 composed of Tim17b isoforms along with DnaJC19, whereas translocase A is nonessential and has a central role in oncogenesis. Translocase B, having a normal import rate, is essential for constitutive mitochondrial functions such as maintenance of electron transport chain complex activity, organellar morphology, iron-sulfur cluster protein biogenesis, and mitochondrial DNA. In contrast, translocase A, though dispensable for housekeeping functions with a comparatively lower import rate, plays a specific role in translocating oncoproteins lacking presequence, leading to reprogrammed mitochondrial functions and hence establishing a possible link between the TIM23 complex and tumorigenicity.

Normal cellular function requires homeostatic counterbalance of various metabolic pathways, with mitochondria playing a central role in the complex processes. Proper mitochondrial function requires a plethora of different proteins, which are recruited into the organelle through well-defined inner membrane protein translocation machinery (1–3). The presequence translocase or the TIM23 complex accounts for import of approximately 60% of the total mitochondrial proteome and hence is critical for mitochondria biogenesis (4). In yeast, the subunit organization and functional annotations of the machinery are well established and show the presence of a single translocase performing the matrix-directed protein translocation. The yeast presequence translocase consists of a core channel composed of Tim23 along with Tim17. Both Tim23 and Tim17 are essential and form the channel component for the entry of the polypeptide chain. Nonessential accessory proteins, such as Tim21 and Pam17, are involved in conserved interactions with the core components and are important in the maintenance of the overall organization of the machinery. The TIM23 core channel is involved in a cooperative interaction with the matrix-directed import motor (composed of mtHsp70, Tim44, Mge1, and the Pam18-Pam16 subcomplex) in driving the import process (1, 2, 5–9). Tim23 and Tim17 form the central channel and along with Tim50 are involved in presorting the incoming polypeptide chains (1, 2, 4, 10) into the channel.

The initial translocation across the machinery is inner membrane potential dependent, and the final step is driven by ATPase activity of the import motor (11–13). The mitochondrial Hsp70 (mtHsp70), with the aid of accessory factors such as J-proteins, plays a critical central role during the process. It captures the incoming polypeptide chain and internalizes it into the matrix. Pam18 forms the J-protein counterpart of Hsp70 and stimulates the rate of ATP hydrolysis of mtHsp70. Pam16 is a J-like protein which forms a heterodimeric subcomplex with Pam18 via the J-domains and inhibits the ATPase stimulatory activity of Pam18. Recruitment of Pam18 to the translocase occurs via its subcomplex formation with Pam16. On the other hand, the intermembrane space (IMS) region of Pam18 interacts with the Tim17 C-terminal region, though this association is not critical for its recruitment to the channel.

Although the existence of such analogous machinery is predicted in the mammalian mitochondria (14), its intricate architecture in humans with complex mitochondrial function is still an open question. It is difficult to contemplate the existence of similar machinery in mammalian mitochondria, which are involved in a variety of elaborate functions. Apart from regulating multiple metabolic pathways, human mitochondria have been implicated in various aspects, such as tumorigenicity, apoptosis, and neurodegenerative disorders. Besides, mitochondria are also required for the integration of cellular responses to xenobiotic stress that involves targeting and assembly of specific proteins to determine the phenotype (15–18). Human presequence translocase subunits were identified as proteins associated with mutations and regulated expressions in different cancer subtypes, thus highlighting the possibility of a direct role of the presequence translocase activation in neoplastic transformation (19–26). Based on these observations, we tried to elucidate how the translocase components are organized in the inner membrane and regulate the import of

diversified substrates in order to maintain the mitochondrial protein homeostasis and assist in reprogramming of the organellar functions.

In this report, we reveal the intricate architecture of human inner membrane presequence translocase and provide mechanistic insights on regulation of translocase activity by J-proteins. We have classified the translocases based on their constitutive and supportive function in the maintenance of normal mitochondrial processes. In addition, our work provides the first evidence for the existence of a dedicated translocase for translocation of proteins lacking a mitochondrial signal sequence, which plays an additional role in maintenance of a higher mitochondrial DNA copy number in tumor cells, leading to uncontrolled cancer cell proliferation.

MATERIALS AND METHODS

Cells and cell culture. HEK293T, HeLa, PC-3, OVCAR-3, MCF7, IBR-3, and HaCaT cells were cultured in Dulbecco's modified Eagle's medium containing 10% fetal bovine serum and 1% penicillin-streptomycin. LNCaP cells were grown in RPMI 1640 medium supplemented with the components listed above. Transfection of the cells with the expression constructs was carried out using Lipofectamine 2000 (Invitrogen) as per the manufacturer's instruction and allowed to express for 48 h.

CoIP and immunoblot analysis. For Western analysis, cells were lysed using RIPA buffer (50 mM Tris-Cl [pH 7.4], 150 mM NaCl, 1% NP-40, 0.25% sodium deoxycholate, 1 mM phenylmethylsulfonyl fluoride [PMSF]) containing protease inhibitors cocktail (Sigma). Protein content was estimated by Bradford assay (Bio-Rad) prior to separation on polyacrylamide gels. Mitochondria were isolated using a cell mitochondrion isolation kit (Sigma). Equivalent amounts of purified mitochondria were lysed in translocase coimmunoprecipitation (CoIP) buffer (25 mM Tris [pH 7.5], 10% glycerol, 80 mM KCl, 5 mM EDTA, and 1 mM PMSF) containing 1% digitonin (Calbiochem) or 1% Triton X-100 (U.S. Biochemicals) as mentioned, followed by clarification at $20,000 \times g$ for 20 min. The supernatant was subjected to CoIP using the respective antibody-conjugated beads in accordance with the experiment. The immunoprecipitated complexes resolved on denaturing gel were transferred to polyvinylidene difluoride (PVDF) (Millipore) and developed through Western Lighting ECL (PerkinElmer).

RNA interference (RNAi) knockdown experiments. HEK293T cells were seeded in Opti-MEM (Invitrogen) and transfected with the following 5 μM duplex small interfering RNA (dsiRNA) pools: HSC.RNAI.N016069.12.1 and HSC.RNAI.N016069.12.2 (IDT) for *MAGMAS*, HSC.RNAI.N001190233.12.5 and HSC.RNAI.N001190233. 12.7 (IDT) for *DNAJC19*, HSC.RNAI.N006335.12.1 and HSC.RNAI. N006335.12.2 (IDT) for *TIM17A*, ON-TARGETplus SMART pool (Dharmacon) for *DNAJC15*. Transfection was performed using Lipofectamine 2000 (Invitrogen) by following the manufacturer's instructions. Hep1 was used as a mitochondrial loading control and Tim23 as a control for translocase integrity.

BN-PAGE. Blue native (BN) electrophoresis was essentially carried out as described previously (14). Briefly, 100 μg of yeast or human mitochondria was solubilized in 1% digitonin (Calbiochem) containing buffer and further clarified by centrifuging at $20,000 \times g$ for 20 min. The samples were diluted in 0.2% Coomassie blue G-250 and 5 mM aminocaproic acid and were separated in a 6 to 16.5% gradient native gel. The complexes were transferred onto a PVDF membrane and detected by immunoblotting using specific antibodies. The size of the individual complexes was determined based on the mobility pattern of a native protein molecular weight standard. Similarly, to decipher the oligomeric state of the proteins, the relative migration of the bands was mapped onto the molecular weight standard.

Glycerol gradient centrifugation. A total of 2 mg of yeast or human mitochondria was lysed in 1% digitonin buffer (25 mM Tris [pH 7.5], 10% glycerol, 80 mM KCl, 5 mM EDTA, and 1 mM PMSF). After centrifugation at $20,000 \times g$ for 20 min, the supernatant was layered onto a 20 to 50% glycerol gradient containing 5 mM aminocaproic acid and centrifuged at $160,000 \times g$ for 16 h. The samples were aspirated from the top, and the fractions were analyzed by immunoblotting.

Fluorescence imaging in live cells. MCF7 or LNCaP cells were seeded on coverslips and dual transfected with the plasmid of interest and construct expressing mtDsRED. The transfection was performed using Lipofectamine 2000, and the proteins were allowed to express for 52 h. Images were acquired by Zeiss AxioObserver Z1 Apotome 2.0 63× oil numerical aperture (NA) 1.45 Optovar 1 at 25°C. The images were captured using a Zeiss AxioCam MRm camera and processed using Zeiss Axio Vision Rel. 4.8 software.

Antibody preparation. The following antibodies were used for primary detection: anti-Tim23 (1:5,000; BD Biosciences), anti-Tim44 (1: 1,000; BD Biosciences), anti-Tim17a (1:2,500; Epitomics), anti-Tim50 (1:750; Imgenex Biotech), and antiactin (1:20,000; Sigma); anti-Magmas, anti-DnaJC15, and anti-DnaJC19 antibodies, generated by injecting their corresponding J-domain fragments; and anti-Hep1, raised against the full-length proteins at Imgenex Biotech. Antibody against human Tim17b was raised against the C-terminal peptide CPKDGTPAPGYPSYQ, which is common for both isoforms. Hence, anti-Tim17b antibody could detect and pull down both Tim17b1 and Tim17b2 in CoIP and immunodetection assays. Anti-p53 and anti-PCNA were a kind gift from Sathees Raghavan, and anti-Erk2 was gifted by Rudriah Medhamurthy, Indian Institute of Science, Bangalore, India. Antibodies specific to yeast presequence translocase components, namely, Tim44 (27), Tim23, Pam18, and Pam16 (17), were generated as described. Antisera against yeast Tim50, Tim21, and Tim17 were generated against the CLPEAPSSQPLQA peptide for Tim17 and the C-terminal IMS domain for Tim50 (amino acids [aa] 133 to 476) and Tim21 (aa 102 to 240) (Imgenex Biotech). For coimmunoprecipitation analysis, antisera were affinity purified and cross-linked to either protein A or protein G beads (GE Healthcare). Secondary immunodecoration was performed using horseradish peroxidase (HRP)-conjugated anti-rabbit or anti-mouse IgG (GE Healthcare).

Cell viability and cell proliferation. The percentage of viable cells was determined by 3-(4,5-dimethylthiazol-2-yl)-2,5-diphenyltetrazolium bromide assay (MTT assay) (Invitrogen) as instructed in the manufacturer's manual.

Kinetics of protein import. Protein import activity of individual translocases was quantified using isolated mitochondria by assessing the mitochondrial localization of model recombinant substrates created by fusing the N-terminal presequence of cytochrome b_2 (Cytb$_2$) with the nucleus-localized protein dihydrofolate reductase (DHFR). Import assays were carried out utilizing three purified recombinant substrates, namely, Cytb$_2$(47)-DHFR as a matrix-localized substrate, Cytb$_2$(167)-DHFR for precursor proteins sorted into the inner membrane, and Cytb$_2$(167Δ19)-DHFR lacking the 19-aa transmembrane region as another matrix-localized protein. The relative kinetics of protein import was assayed as described previously (28) except for minor modifications. The amount of mature protein imported into the organelle was quantified by ImageJ 1.43u and plotted using GraphPad Prism5.

Determination of mitochondrial DNA copy number. The copy number variation in mitochondrial DNA was determined by subjecting the total cellular DNA to quantitative real-time PCR by using an iQ5 multicolor real-time PCR detection system (Bio-Rad). The primer sequences used for amplifying the gene segments were as follows: for mitochondrial NADH dehydrogenase subunit I (ND1), ND1-F, 5′-CTAGCC ATCATTCTACTATCAAC-3′, and ND1-R, 5′-AGGAGTAATCAGAGG TGTTC-3′; for cytochrome oxidase subunit II (CO2), CO2-F, 5′-TGCT TCCTAGTCCTGTATG-3′, and CO2-R, 5′-GCGTCTGAGATGTTAGT ATTAG-3′. The reactions were normalized by amplification of nuclear DNA controls, namely, cyclophilin B (CypB) with primer sequence, Cyp B-F, 5′-ACCTACGAATTGGAGATGAA-3′, and CypB-R, 5′-CCTTGAT TACACGATGGAATT-3′; β-actin with primer sequence, β-actin-F, 5′-T

CCCAGCACACTTAACTTAGC-3′, and β-actin-R, 5′-AGCCACAAGA AACACTCAGG-3′. Relative copy number was calculated from the threshold cycle value (C_T value) using the $\Delta\Delta C_T$ method as described previously (29). Each reaction was optimized, and the linearity was confirmed within an appropriate concentration range using genomic DNA from a normal kidney epithelial cell line, HEK293T.

As a second approach to comparatively quantify the mitochondrial DNA content, we utilized a fluorometric assay system where a corresponding increase in Sybr green (Molecular Probes, Invitrogen) fluorescence due to higher DNA binding was quantified as a measure of the amount of DNA content. Equivalent amounts of control and small interfering RNA (siRNA) knockdown mitochondria were incubated with saturating amounts of intrinsically nonfluorescent Sybr green dye. A lambda scan (500 nm to 650 nm) was carried out to quantify the relative fluorescence increase due to higher organellar DNA-dye binding over the spectra.

Measurement of mitochondrial membrane potential. HEK239T cells were transfected with control siRNA and siRNA corresponding to Tim17a, Tim17b, or both. The mitochondrial membrane potential was assessed by JC-1 dye, which accumulates inside the mitochondria in a potential dependent manner to form J-aggregates. The oligomeric J-aggregates fluoresce at the red region of the spectra (λ_{590}) compared to the cytosolic green fluorescence (λ_{530}). The ratio of mitochondrial red and cytosolic green fluorescence is proportional to the maintenance of mitochondrial inner membrane potential. After 48 h of incubation, the cells were stained with 2 nm JC-1 for 15 min and subjected to an emission wavelength scan from 500 nm to 620 nm by using a Tecan Infinite 200 Pro spectrofluorometer. The fluorescence intensity of red emission maxima (λ_{590}) due to mitochondrial localization of the dye, over cytosolic green (λ_{530}), was quantified to determine the integrity of membrane potential.

Analysis of mitochondrial morphology. HeLa cells were transfected with the plasmid containing mitochondrially targeted DsRed (mtDsRed). Twenty-four hours posttransfection, the cells were retransfected with corresponding siRNA and incubated for 48 h prior to imaging by Zeiss AxioObserver Z1 Apotome 2.0 63× oil NA 1.45 Optovar 1.6 at 25°C. The images were acquired by using a Zeiss AxioCam MRm camera and processed using Zeiss Axio Vision Rel. 4.8 software. Digitally zoomed images were created as an inset using Adobe Photoshop 7.0.

Measurement of the activities of electron transport chain complexes. The activities of ETC complexes were assessed in isolated mitochondria based on a method described previously (30). Briefly, for complex I activity, mitochondria were incubated in phosphate buffer containing 2 mM sodium azide and 1 mM NADH. The reaction was initiated by adding 60 μM ubiquinone. The decrease in absorbance at 340 nm was recorded for 2 min. Specificity of the reaction was checked by inhibiting complex I with rotenone. Complex II activity was measured by incubating isolated mitochondria in phosphate buffer containing 2 μg/μl rotenone, 2 μg/μl antimycin A, 2 mM sodium azide, and 65 μM ubiquinone. The reaction was initialized by adding 50 μM dichlorophenolindophenol (DCPIP), and the decrease in absorbance was recorded for 2 min. For the measurement of complex III activity, mitochondria were incubated in a phosphate buffer along with 2 mM sodium azide, 0.025% (vol/vol) Tween 20, and 75 μM oxidized cytochrome *c*, 0.1 mM ubiquinol was added to initiate the reaction, and an increase in absorbance was observed at 550 nm. To confirm the specificity of the reaction, mitochondria were separately incubated with antimycin A. To measure complex IV activity, the oxidation of reduced cytochrome *c* was measured via the decrease in absorbance at 550 nm. Sodium azide, an inhibitor of complex IV, was used to check the specificity of the reaction.

Assessment of Fe-S cluster protein biogenesis. To assess the biogenesis of Fe-S cluster proteins, activity of a model Fe-S cluster containing enzyme aconitase was measured. Isolated mitochondria were permeabilized using 0.1% deoxycholic acid, and the reaction was initiated with 2.5 mM citrate. The increase of absorbance at 240 nm was recorded for 2 min.

Quantification of mitochondrial ATP levels. The level of cellular respiration was quantified by measuring the mitochondrial ATP levels by using isolated mitochondria with the mitochondrial ToxGlo assay kit (Promega) as per the manufacturer's instructions.

Determination of cellular ROS levels. Cells were stained with 2′,7′-dichlorodihydrofluorescein diacetate (H_2DCFDA) (Molecular Probes, Invitrogen) to measure the total cellular reactive oxygen species (ROS) levels. The increase in fluorescence corresponding to higher ROS levels was detected through flow cytometry with an excitation/emission wavelength of 495/527 nm. The mitochondrial superoxide levels were quantified by labeling the cells with the superoxide-sensitive dye MitoSOX (Molecular Probes, Invitrogen), followed by flow cytometric detection at an excitation/emission wavelength of 510/580 nm.

Analysis of DNA replication. Cellular DNA replication was measured as relative incorporation of [³H]thymidine. Briefly, cells were transfected with siRNA and incubated for 36 h. A total of 0.5×10^6 untransfected or transfected cells was incubated with 1 μCi of [³H]thymidine for 30 min. The cells were extensively washed with 1× phosphate-buffered saline (PBS) and fixed in 70% methanol. The amount of [³H]thymidine incorporation was quantified by measuring the scintillation counts in a PerkinElmer liquid scintillation counter.

Statistical analysis. Calculation of statistical significance was done using a two-tailed Student *t* test through GraphPad Prism5 software unless otherwise mentioned; *P* values are mentioned in figure legends.

RESULTS

Subunit organization of human mitochondrial presequence translocase. The yeast mitochondrial translocation machinery is well characterized, and numerous reports have dissected the conserved interaction between different translocation components during the translocation process. In contrast to yeast, sequence analysis of the human mitochondrial proteome suggests the presence of two paralogs of the Tim17 central channel component, namely, Tim17a and Tim17b. Tim17b in turn has two isoforms, Tim17b₁ and Tim17b₂. To uncover the subunit organization of presequence translocase in humans, we analyzed mitochondria isolated from HEK293T cells and compared them with the well-studied yeast system (2, 14). We utilized three different techniques, namely, glycerol gradient centrifugation, blue native PAGE (BN-PAGE), and coimmunoprecipitation (CoIP) analysis. It has been established beyond doubt that resolution of digitonin-processed yeast mitochondrial extract on glycerol gradient centrifugation results in recovery of all the channel components from fractions corresponding to 240 kDa in size (14, 15). This indicates that yeast mitochondria consist of a single Tim23-translocase complex of 240 kDa. In comparison, the distribution among the channel components in humans was found to be completely different. Human Tim23-translocase components, namely, Tim23, Tim50, Tim44, Tim21, and Magmas, separated into three distinct peaks with molecular sizes of ~200, ~240, and ~450 kDa (Fig. 1A and B), and the subunits were found to be distributed equivalently in all three peaks. However, a major difference existed in the subunit distribution pattern of Tim17 and J-protein paralogs. Immunodetection with specific antibodies revealed that the Tim17a paralog and DnaJC15 (JC15) overlapped with the 240-kDa peak region, while Tim17b₂ and Tim17b₁ isoforms were retrieved from the 200- and 450-kDa fractions together with DnaJC19 (JC19) (Fig. 1B).

As a second approach, the digitonin-lysed human mitochondria were resolved through BN-PAGE and compared with the yeast system. Upon BN-PAGE analysis, yeast mitochondria showed a presence of three distinct complexes of the sizes ~90
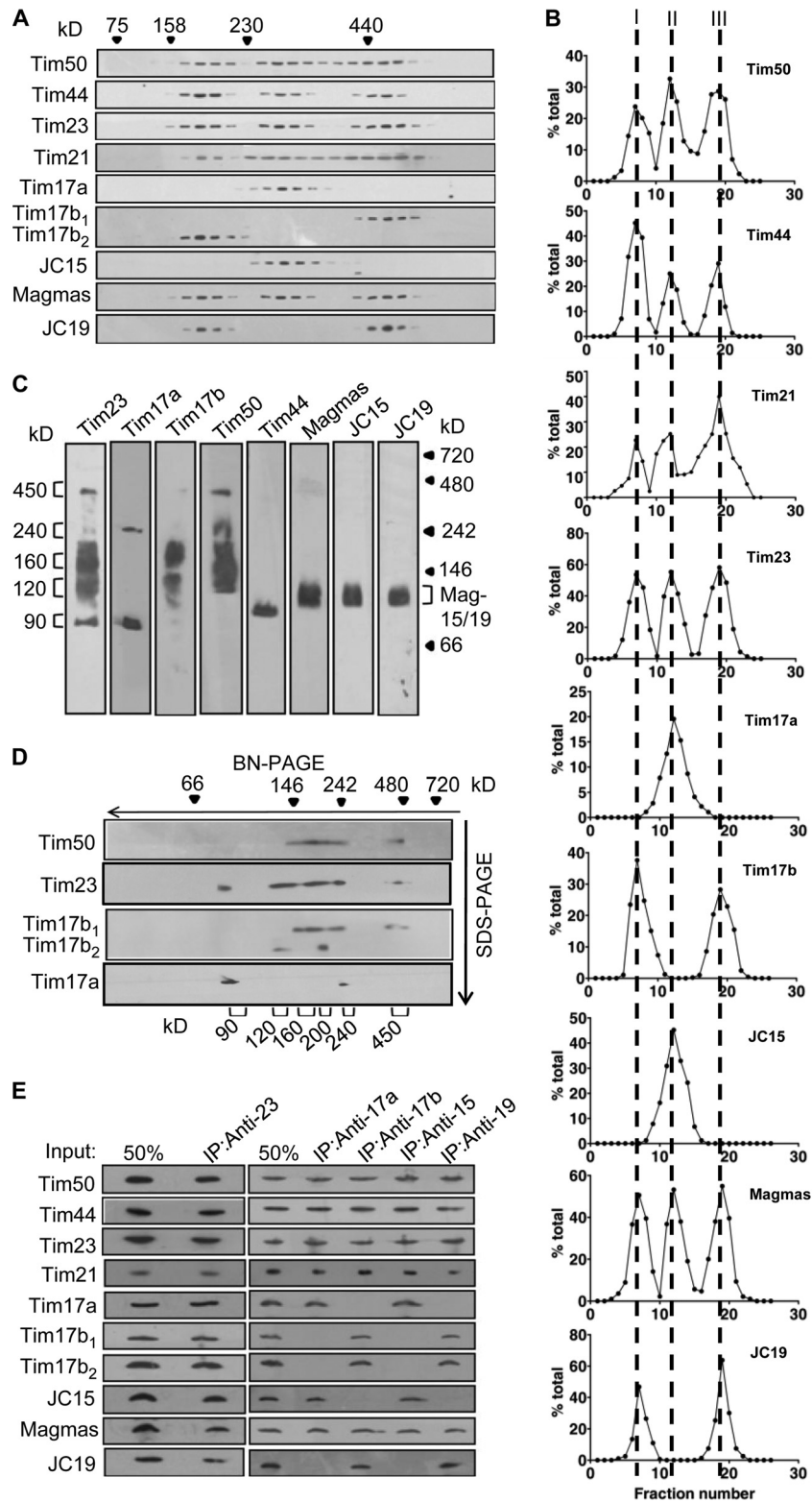
FIG 1 Organization of human inner membrane translocase. (A) HEK293T mitochondria were solubilized in 1% digitonin buffer and analyzed by glycerol gradient centrifugation (20 to 50%). The fractions were aspirated from the top and immunoblotted sequentially. (B) The bands were densitometrically quantified and are represented as a line graph. Peaks corresponding to individual translocases are denoted by dotted lines. (C) Blue native electrophoresis (BN-PAGE) of digitonin-lysed HEK293T mitochondria. After electrophoresis, the gel strips were cut and immunodecorated with specific antibodies. The size of the individual complexes was determined based on the mobility pattern of the native protein molecular weight standard. (D) The components of distinctive complexes were further resolved for improved clarity via two-dimensional BN-PAGE, followed by immunodetection. (E) For CoIP of the TIM23 complex, 250 μg of mitochondria was digitonin lysed and subjected to CoIP using the indicated antibodies. The samples were analyzed by antibodies against the translocase components.

kDa, 146 kDa, and 240 kDa. However, the separation of translocase components into three peaks in the glycerol gradient centrifugation indicated a possibility for human BN profiles to be different from that of yeast. Immunodecoration of BN-PAGE blots of the human counterparts revealed the presence of additional larger complexes of molecular sizes ranging from 120, 160, 200, and 450 kDa formed by Tim23 together with $Tim17b_1$ and $Tim17b_2$ isoforms (Fig. 1C). On the other hand, Tim23-Tim17a forms classical 90- and 240-kDa complexes similar to the yeast system (Fig. 1C) (31, 32). Furthermore, the complexes detected through Tim17b immunoblotting overlapped with the 120-, 160-, 200-, and 450-kDa complexes visualized by Tim23 antibodies (Fig. 1C). For better identification of translocase components, the complexes were further separated on two-dimensional BN-PAGE gels. Interestingly, the $Tim17b_1$ isoform comigrates with the larger ~160- and ~450-kDa complexes, while $Tim17b_2$ comigrates with the smaller ~120- and ~200-kDa complexes (Fig. 1D). This suggests that the smaller Tim17 isoform $Tim17b_2$ forms the smaller translocase of ~200 kDa; the larger Tim17 isoform, $Tim17b_1$, constitutes the translocase of ~450 kDa. Tim17a comprises part of the ancestral translocase of ~240 kDa, corresponding to that of yeast. These findings clearly highlight that the organization of presequence translocase of the human inner mitochondrial membrane is very intricate, and core channel composition of the translocase is determined primarily by the presence of Tim17a and Tim17b isoforms.

To validate the nature and integrity of translocase complexes, digitonin-lysed human mitochondrial lysates from HEK293T were subjected for CoIP analysis. To confirm our CoIP results obtained from HEK293T cells, we performed a similar pulldown assay using mitochondrial lysate from cell lines of another noncancerous origin, such as HaCaT and IBR3 (data not shown). As anticipated, Tim23, being the common component of different translocases, immunoprecipitates all the subunits of the translocases, including both Tim17 and J-protein paralogs (Fig. 1E). However, CoIP using Tim17a-specific antibody resulted in precipitation of the core subunits, including Tim17a, Magmas, and JC15. At the same time, no immunoprecipitating bands of Tim17b and JC19 were detected. On the contrary, we observed that Tim17b antibody coimmunoprecipitates core complex subunits, including Magmas and JC19, but does not immunoprecipitate Tim17a and JC15 (Fig. 1E). The association of J-proteins with separate translocases was further confirmed by CoIP using JC19- and JC15-specific antibodies. JC19 coprecipitates with the translocase complex containing Tim17b isoforms, while JC15 was found to be associated with Tim17a translocase (Fig. 1E). This indicates that the J-proteins are recruited specifically to each translocase, with Magmas forming the common central component. In summary, the human inner mitochondrial membrane possesses three distinct Tim23 complexes constituting two separate J-proteins: translocase A being distinguished by the presence of the Tim17a paralog with JC15, while translocase B1 and translocase B2 consist of $Tim17b_1$ and $Tim17b_2$, respectively, in complex with the JC19 subunit.

Recruitment of J-proteins at the presequence translocase by Magmas. Our previous report suggests a formation of a heterodimeric subcomplex by JC19 with Magmas, and mutations in Magmas cause dissociation of the J-protein from the translocon (16). Therefore, we tested the idea of whether Magmas, being the central critical component of the PAM subcomplexes, is responsible

for managing the differential association of the J-proteins with the channel. To address the dynamic recruitment of J-proteins and how they achieve their functional specificities at the three specific translocases, Magmas-, JC19-, and JC15-depleted mitochondrial lysates (Fig. 2B) were subjected to translocase CoIP analysis and probed for the recruitment into the core translocase complex. JC15 depletion did not disrupt the interaction of Magmas with the translocation machinery, and neither did the association of JC19 with the respective translocase B1 and translocase B2 (Fig. 2A1). Though no association of JC15 with translocase A was observed in JC15-silenced cells, pulldown of the translocation complex by Tim17a antibodies resulted in immunoprecipitation of JC19, indicating a partial recruitment of JC19 into the translocase A complex, which was not observed in untransfected controls (Fig. 2A2). Similarly, under JC19-silenced conditions, a fractional association of JC15 was observed with translocases B1 and B2 in the absence of JC19, when immunoprecipitation was done using Tim17b-specific antibody (Fig. 2A3). The association of Magmas with the translocases remained unaltered. We hypothesized that Magmas mediates such a nonspecific recruitment of JC15 and JC19 into the translocase as a subcomplex by partially competing for the binding to the channel under individual J-protein-depleted conditions. To address this phenomenon of mutual recruitment of respective J-proteins in depleted cells, Magmas-silenced cell lysates were subjected to CoIP. Magmas-silenced cells did not alter the association of the majority of core complex components. However, the association of JC19 and JC15 to their respective translocases was completely impaired in the absence of Magmas, as indicated by anti-Tim23, Tim17a, and Tim17b immunoprecipitation (Fig. 2A, panels 1 to 3). These results provide direct evidence for Magmas playing a most critical role in the tethering and redistribution of J-proteins to the specific translocases as part of the subcomplex.

Alterations in Magmas expression cause redistribution of J-proteins at the translocases. In yeast, it has been demonstrated that mutations in the Magmas J-domain result in dissociation of Pam18 from the translocation machinery (17). However, in humans, Magmas was found to play an additional role in cross-recruitment of J-proteins to either of the translocases, and elevated amounts of the protein have been observed in cancer subtypes. Therefore, to further validate the role of Magmas in redistribution of J-proteins at the import channel and understand the effect of Magmas overexpression in distribution of J-proteins, we mimicked the situation of higher cellular levels of Magmas by overexpressing the protein in HEK293T cells (Fig. 2C). Upon CoIP analysis, we found that overexpression of Magmas at the translocase did not have any effect on the association of the other translocase components, though enhanced recruitment of Magmas was observed with the channel, as indicated by CoIP using Tim23-specific antibodies (Fig. 2D, panel 1). Interestingly, CoIP using Tim17a antibodies resulted in a partial pulldown of JC19 with the translocase A component along with JC15 (Fig. 2D, panel 2). Similarly, CoIP with Tim17b-specific antibodies showed recruitment of both JC15 and JC19 to translocase B1 and B2 (Fig. 2D, panel 3). This indicates that Magmas mediates a cross-recruitment of J-proteins at the channel under overexpressed conditions.

Previous proteomic studies have shown the presence of an elevated amount of Magmas in various cancer subtypes, such as neoplastic prostrate and pituitary adenomas (18, 19). Therefore, to demonstrate how enhanced levels of Magmas modulate the
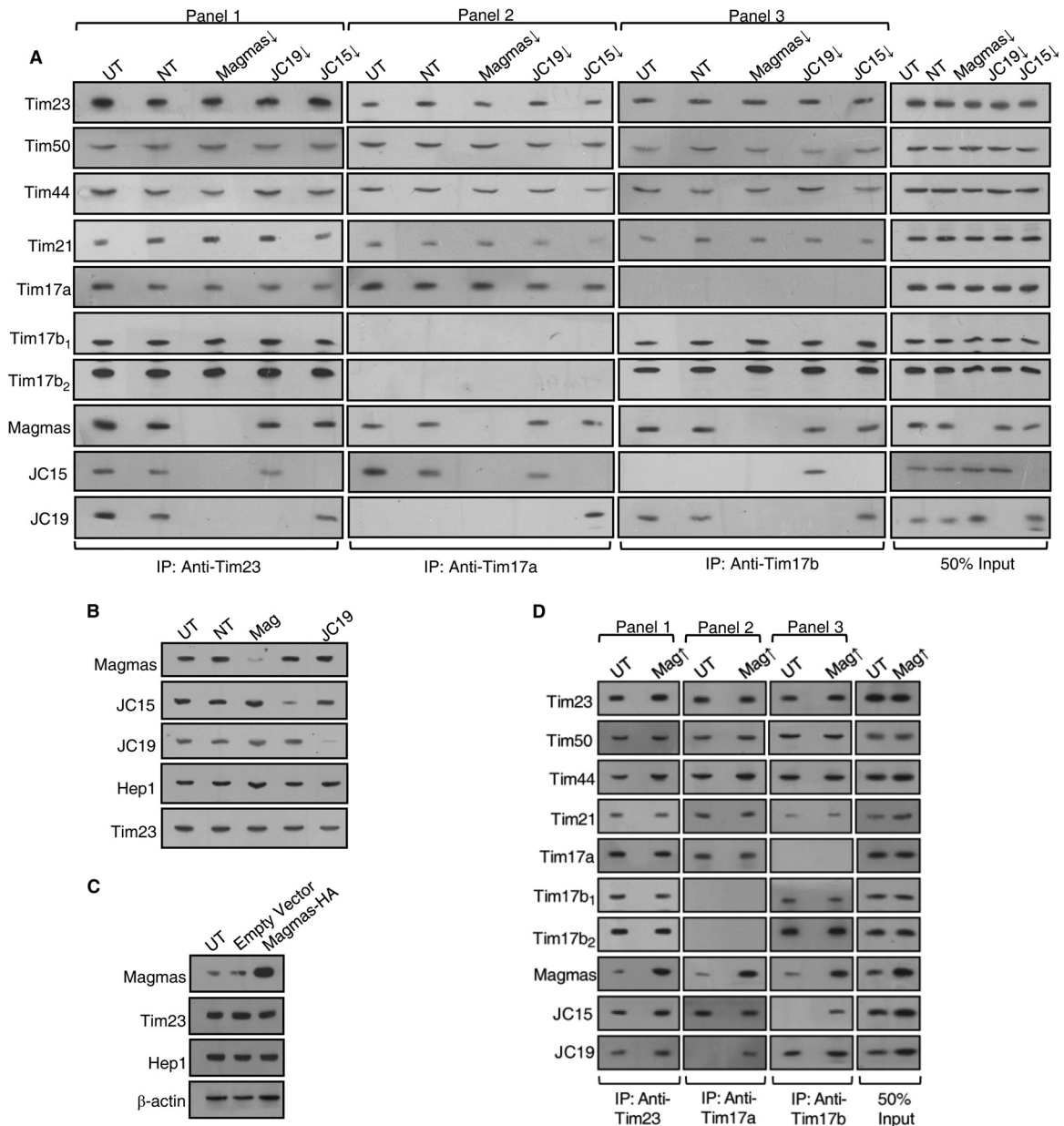
FIG 2 Recruitment of J-proteins at presequence translocase through Magmas. (A) HEK293T mitochondria depleted for Magmas (Mag), JC19, or JC15 were digitonin lysed and subjected to CoIP using the indicated antibody-conjugated beads, followed by immunoblot analysis. (B) Transfection of HEK293T cells was carried out using siRNA against Magmas, JC15, and JC19. After 48 h, the cells were lysed and subjected to immunoblot analysis. (C) HEK293T cells were transfected with construct overexpressing Magmas and incubated for 48 h, followed by immunoblotting with anti-Magmas antibodies. (D) Mitochondria isolated from HEK293T cells overexpressing Magmas were lysed and incubated with the indicated antibody beads. Translocase complex-bound antibody beads were immunoblotted with specific antibodies against the translocase components. UT, untransfected control; NT, transfected with nontargeting dsiRNA as the internal control; ↓, mRNA downregulated by dsiRNA; ↑, overexpression of Magmas.

translocase composition in cancer cells, we utilized mitochondria isolated from neoplastic prostate-derived cell lines (PC-3 and LNCaP) that intrinsically overexpressed Magmas (Fig. 3A) and subjected them to CoIP analysis. We observed that consistent with our earlier data, CoIP using Tim23 antibodies showed an increased pulldown of Magmas with the translocases (Fig. 3B, panel 1). Interestingly, overexpression of Magmas promoted the recruitment of JC15 as well as partially JC19 to translocase A (Fig. 3B, panel 2). A similar distribution in the recruitment of J-pro-

teins was observed for translocases B1 and B2 upon CoIP with Tim17b antibody, where JC15 was recruited along with JC19 (Fig. 3B, panel 3). This suggests that Magmas plays a significant role in altering the relative activities of the translocases in overexpressed conditions. Intriguingly, both the cancer-derived cell lines showed intrinsically overexpressed components of the primitive translocase A, such as Magmas, Tim50, Tim44, and Tim17a (Fig. 3B), indicating that translocase A might have a potential role in oncogenic transformation. However, the cross-recruitment of J-
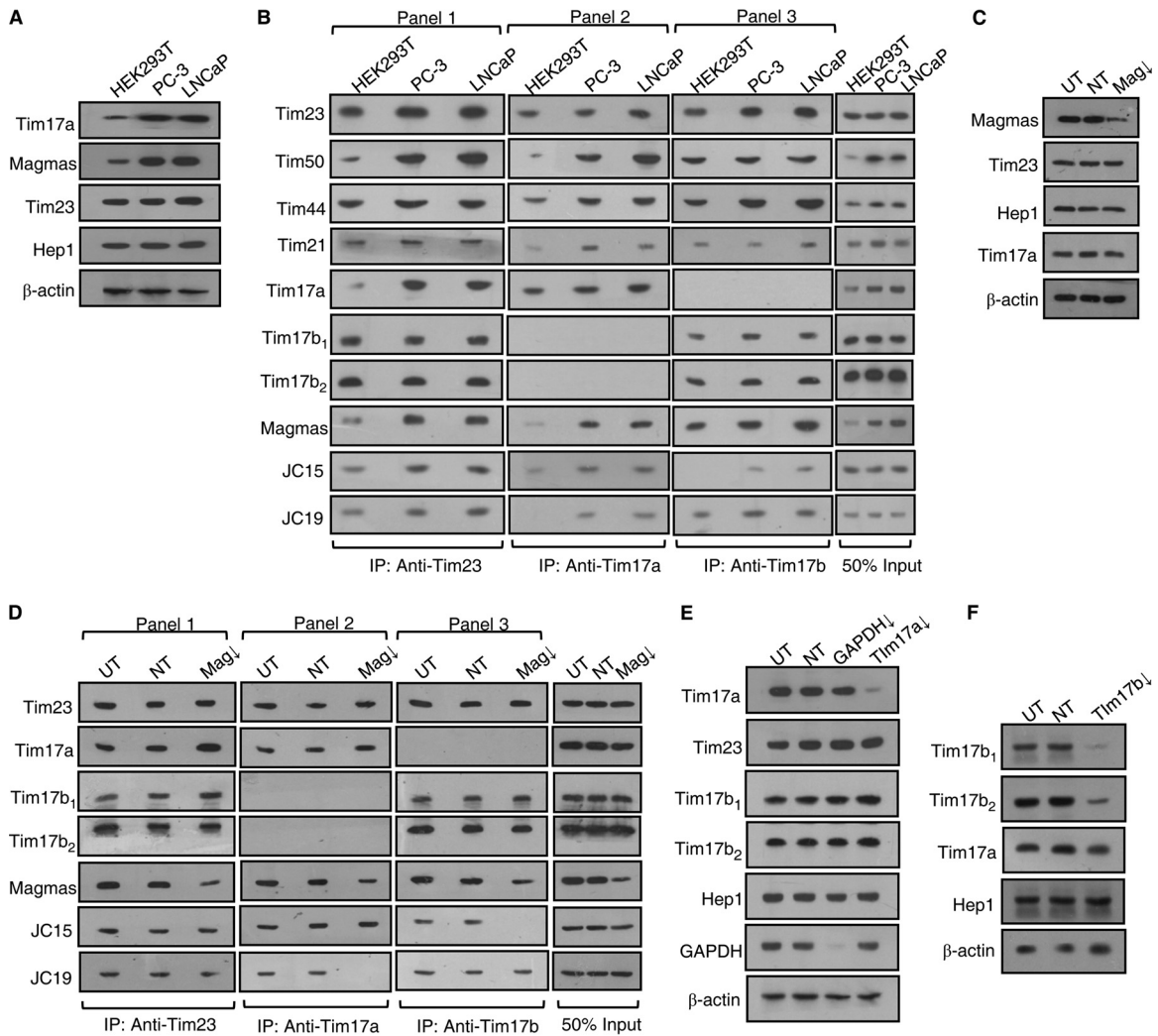
FIG 3 Altered Magmas levels redistribute J-proteins at the translocase channel in LNCaP cells. (A) Equivalent amounts of mitochondria isolated from HEK293T, PC-3, and LNCaP cells were analyzed by immunoblotting using the indicated antibodies. (B) Equivalent amounts of mitochondrial lysate from HEK293T, PC-3, and LNCaP cells were incubated with specific cross-linked antibodies, followed by immunoelectrophoresis. (C) LNCaP cells were transfected with siRNA specific for Magmas and incubated for 30 h, followed by immunoblotting using anti-Magmas and the indicated control antibodies. (D) LNCaP cells having reduced Magmas expression up to normal levels were subjected to immunoprecipitation using specific antibody-conjugated beads. The immunoprecipitates were detected by Western analysis using antibodies for individual translocase components. (E) Immunoblot analysis for protein expression of HEK293T cells transfected with siRNA against Tim17a and incubated for 48 h. (F) HEK293T cells transfected with siRNA specific to Tim17b were subjected to immunoblot analysis to assay the levels of protein expression. UT, untransfected control; NT, transfected with nontargeting dsiRNA as the internal control; ↓, mRNA downregulated by dsiRNA.

proteins at the translocases was found to be a function of altered Magmas expression alone and is independent of the levels of other translocase components, since overexpression of Magmas solely in HEK293T cells resulted in redistribution of J-proteins at the translocation channels (Fig. 2D). To further prove this observation, we partially depleted Magmas levels in LNCaP cells (Fig. 3C) and subjected the isolated mitochondria to CoIP analysis. Reduction in Magmas expression resulted in a specific pulldown of JC15 and JC19 with translocases A and B, respectively (Fig. 3D). In summary, the corecruitment of JC15 and JC19 observed with different translocases under Magmas-overexpressed conditions in both HEK293T and cancer-derived cells suggests that Magmas remodels the mitochondrial import activity in tumor cells.

Specificity of J-protein recruitment at the translocase. Since both J-proteins are dynamically recruited to the translocation channel, and their redistribution is mediated by the expression pattern of Magmas, specificity of the J-proteins toward a particular translocation channel remains an intriguing question. It has been well documented in yeast that the N terminus of Pam18 is involved in a conserved interaction with the C terminus of Tim17 (33). Indeed, upon depletion of nonessential component Tim17a (Fig. 3E) and subsequent CoIP analysis, the association of JC15 with the translocase A was significantly reduced, as evident from immunoprecipitation using anti-Tim23 antibodies (Fig. 4A, panel 1). Together, the nonspecific recruitment of JC15 to translocases B1 and B2 was not observed, thus, potentially imparting the specificity in the J-protein recruitment (Fig. 4A, panels 2 and 3).
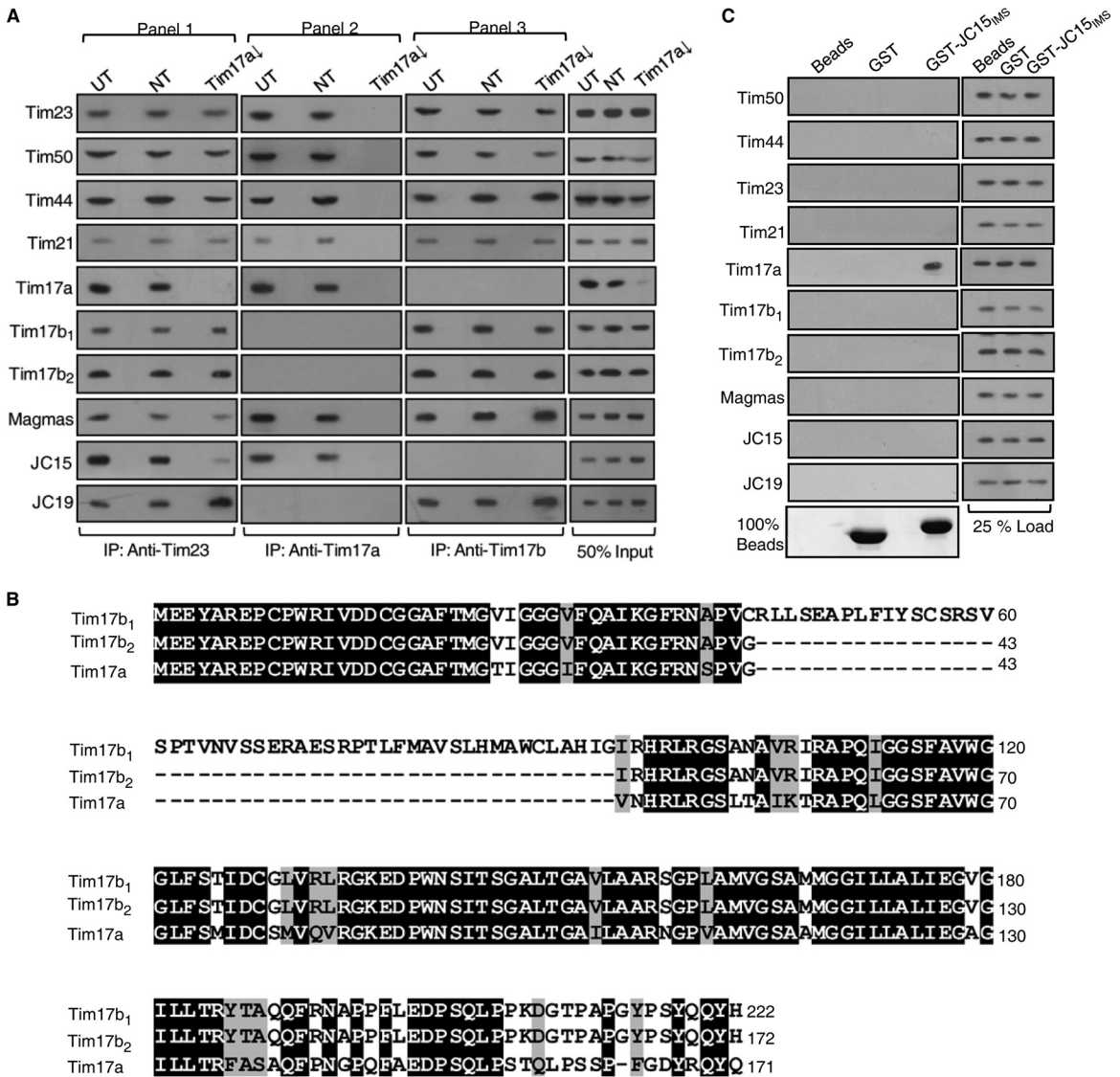
FIG 4 Specificity of JC15 association with translocase A. (A) Mitochondria were isolated from Tim17a-depleted cells and lysed with 1% digitonin. The mitochondrial lysates were subjected to CoIP and analyzed by immunoblotting. (B) Sequence analysis of Tim17a and Tim17b isoforms in human mitochondria. Protein sequences corresponding to the Tim17a (NCBI accession no. NP_006326.1) paralog and the Tim17b₁ (NCBI accession no. NP_001161419.1) and Tim17b₂ (NCBI accession no. NP_005825.1) isoforms were mined from the NCBI database. Multiple sequence alignment was performed using ClustalW software. The identical residues are highlighted in black, and similar ones are in gray. (C) N-terminal 35-amino-acid IMS domain of JC15 fused to GST was immobilized on glutathione-Sepharose beads, prior to incubation with Triton X-100-lysed mitochondria. Samples were immunoblotted using the indicated antibodies.

Therefore, we attempted to identify the region within JC15 that is important for its recruitment to translocase A. A closer analysis of the sequence alignment of the J-proteins and Tim17 paralogs indicates that the Tim17 paralogs have primarily diversified at the C-terminal region, whereas JC15 possesses an additional N-terminal intermembrane space (IMS) domain that is lacking in JC19 (Fig. 4B). So, we hypothesized that the N-terminal IMS domain of JC15 might be mediating its particular interaction with Tim17a. To address this, we purified the glutathione S-transferase (GST)-bound N-terminal 35-amino-acid IMS fragment of JC15 and incubated it with Triton X-100-lysed mitochondria, followed by pulldown analysis. The GST pulldown analysis resulted in a specific pulldown of Tim17a and no other subunits of the machinery.

This indicates that the unique N-terminal IMS-exposed region of JC15 specifically interacts with the C terminus of Tim17a and not Tim17b paralogs or any other translocon components and accordingly provides specificity in self-differentiating the recruitment of JC15 to translocase A (Fig. 4C). Hence, JC15, in addition to subcomplex formation with Magmas, is also involved in a second-site interaction with Tim17a at its N terminus. On the other hand, JC19 lacking such an interacting region does not associate with translocase A and is specifically recruited to translocases B1 and B2 through Magmas.

Relative translocation activity of human presequence translocases. Our findings intriguingly suggest that all three translocases might have evolved to have similar import functions in the

biogenesis of human mitochondria. Therefore, to ascertain their precise role for the maintenance of mitochondrial protein import process, we measured the translocation rates of individual translocases using isolated mitochondria. We utilized three different recombinant precursor substrates corresponding to matrix-targeted preproteins and inner membrane sorted preproteins. The protein translocation activity of translocase A was determined by RNA interference (RNAi)-mediated silencing of Tim17b isoforms in order to deplete the Tim17b protein expression (Fig. 3F), thereby causing dissociation and abrogating the activity of translocases B1 and B2. Similarly, knockdown of Tim17a, leading to reduction of Tim17a protein levels (Fig. 3E), abolishes the translocase A function. A specific reduction in the expression of Tim17a or Tim17b was obtained, and no cross-target effect or upregulation of either of the paralogs was observed, thus providing a direct measure of each of the particular translocase import activities (Fig. 3E and F). To measure the individual translocation activities of human translocases, isolated mitochondria from downregulated cells were incubated with the corresponding purified precursor proteins. A time-dependent accumulation of mature forms of the precursors was monitored. The kinetics of import observed under Tim17a-downregulated mitochondria, signifying activity of translocase B, was found to be similar to that of normal mitochondria for two precursors tested (Fig. 5C, D, F, and H). This indicates that translocase B alone is capable of performing the translocation of substrates into the organelle up to the wild-type level, even in the absence of translocase A.

On the other hand, Tim17b-depleted mitochondria reflecting activity of translocase A showed more than 2-fold-lesser import kinetics for matrix-targeted precursors (Fig. 5A, B, E, and G), highlighting its comparatively lower ability to import substrates than translocase B. This suggests that translocase B forms the core primary translocation machinery for the constitutive import activity, whereas translocase A is dispensable but plays a supportive role in the translocation of preproteins into the matrix. Since the TIM23 complex is also involved in the sorting of inner membrane-associated proteins, we assessed the ability of the human translocases to sort proteins containing a hydrophobic transmembrane sequence into the inner mitochondrial membrane. We observed that the difference between the import rates of translocases A and B is more pronounced in the case of inner membrane sorted proteins (Fig. 5I, K, J, and L) than their matrix-targeted counterparts. This highlights a critical role played by translocase B in the import of proteins into mitochondria. On the other hand, since overexpression of translocase A components and remodeling of translocases' organization by Magmas have been observed in cancer cell subtypes, we assessed import activities in mitochondria isolated from LNCaP cells. In contrast to previous results, translocases A and B were found to share similar translocation activities for matrix-targeted and inner membrane sorted preproteins. Both the translocases, however, showed ~2-fold-lower import activity than unsilenced mitochondria (Fig. 6A to F). This shows that translocases A and B act synergistically in import of precursor proteins in cancer cells. In summary, our findings show that translocation of preproteins across the inner membrane is governed primarily by translocase B, and it forms the primary central machinery for import of precursor proteins in normal human mitochondria. At the same time, both translocases A and B play a cognate role in mitochondrial protein translocation in cancer cells.

Essentiality of translocases in maintenance of normal mitochondrial function. Since both the translocation machineries differ significantly in their overall protein translocation rates, it is conceivable that human translocases might be having contrasting phenotypes on the survivability of cells. Depletion of either Tim17a or Tim17b did not considerably alter the inner membrane potential, whereas knockdown of both the Tim17 paralogs caused dissipation of the mitochondrial potential (Fig. 7A and B), as assessed by potential dependent aggregation of JC-1 dye into the mitochondria. On the other hand, downregulation of Tim17b expression caused a significant decrease in cell viability in HEK293T cells (Fig. 7C) and other cell line types (data not shown) compared to Tim17a depletion. This indicates that translocase B is universally critical for maintenance of cell viability, whereas translocase A is dispensable.

To assess how disruptions of translocase A and translocase B affect the maintenance of mitochondrial functions, we analyzed for the two essential aspects: mitochondrial protein biogenesis and activity of the electron transport chain (ETC) complexes. Mitochondrial protein biogenesis in terms of iron-sulfur protein assembly was assayed by measuring the activity of a model Fe-S cluster enzyme, aconitase. Downregulation of Magmas and translocase B subunits JC19 and Tim17b caused significant loss of enzyme activity, whereas knockdown of translocase A components, namely, JC15 and Tim17a, caused a partial retention of enzyme function (Fig. 7D). This suggests that translocase B plays a critical role for normal mitochondrial Fe-S cluster biogenesis, probably by efficiently importing the constituents of the Fe-S cluster biogenetic pathway. A partial loss of enzyme activity under loss of translocase A function suggests that it may be complementing translocase B function in the constitutive import pathway.

Previous reports have indicated the existence of a close functional connection between ETC complexes and protein translocation machinery (20). To test this idea, the relative activities of the ETC complexes were evaluated under individual translocase-depleted conditions. We observed that Magmas and translocase B depletion caused significant reduction in complex function compared to translocase A disruption, which partly altered the activities of the respiratory complexes (Fig. 7E to H). In addition, the loss of the activities of complex I, complex II, and complex III, containing the Fe-S cluster core, is consistent with our data obtained by the aconitase assay. As a result of the loss of ETC activity, Magmas-, JC19-, and Tim17b-downregulated mitochondria showed a marked decrease in the ATP levels compared to those of the untransfected controls (Fig. 7I), indicating incompetency in the respiratory function. On the contrary, JC15- and Tim17a-altered mitochondria showed approximately 50% reduction in the ATP levels (Fig. 7I), supporting the partial loss of respiratory complex function. This shows that translocase B is critical for the maintenance of a normal respiratory state of the mitochondria, with translocase A having an additional supportive role. In contrast, we observed complete loss of Fe-S cluster biogenesis and complex II activity in LNCaP mitochondria depleted for either Tim17a or Tim17b (Fig. 8A and C). A similar reduction in the activities of ETC complexes I, III, and IV and ATP levels was detected in mitochondria depleted of either of the Tim17 paralogs (Fig. 8B, D, E, and F), though the reduction was not as drastic as observed in the case of HEK293T mitochondria. Together, our results indicate that translocases A and B play a comparable role in determining mitochondrial function in cancer cells.
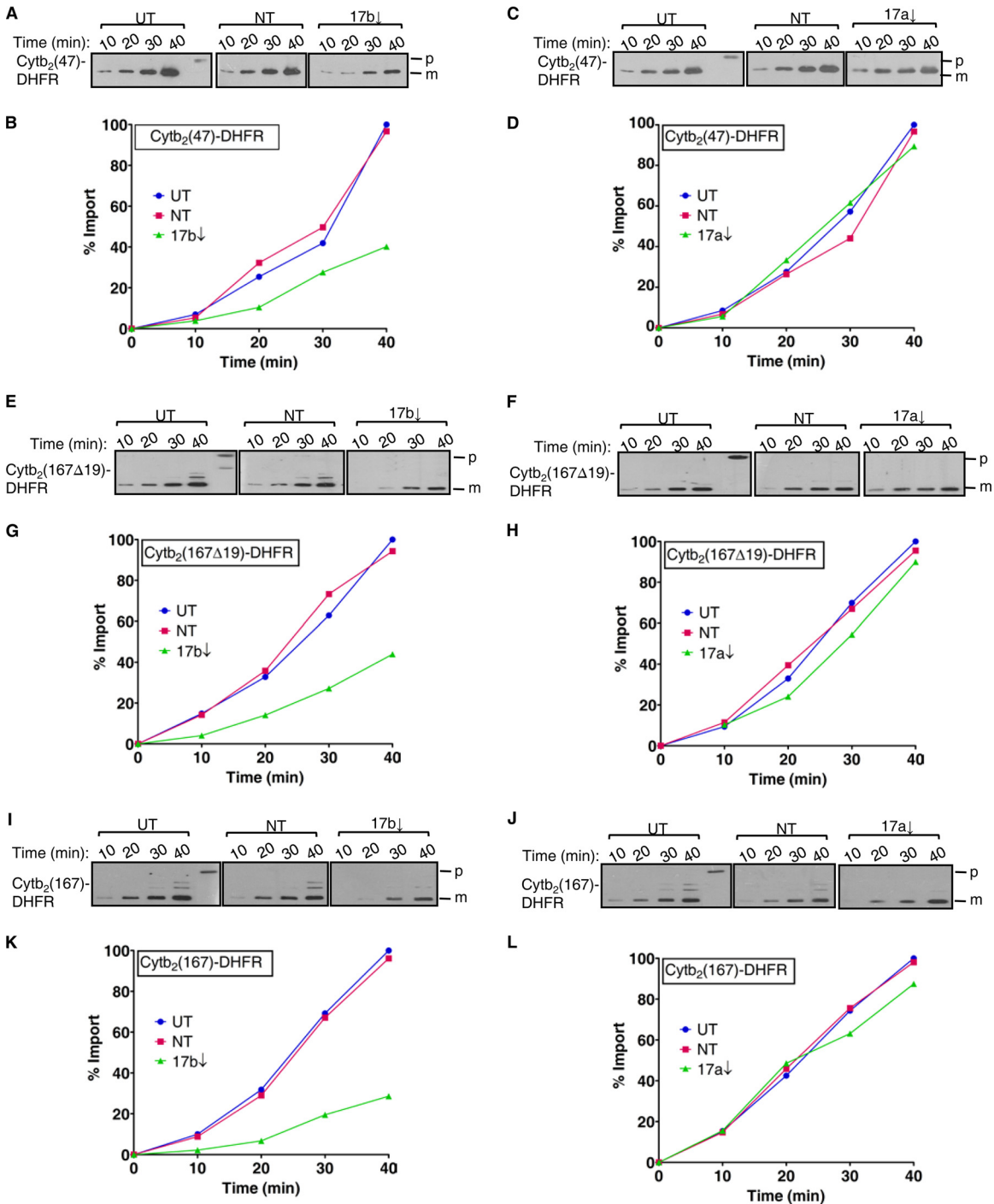
FIG 5 Relative protein translocation activities of human mitochondrial presequence translocation machineries. Protein translocation activity of individual translocase was assessed by subjecting isolated mitochondria downregulated for either of the Tim17 paralogs to three model precursor substrates (p) differing in types of presequences. Mitochondria were isolated from the downregulated cells and subjected to import assay. The accumulation of the intramitochondrial mature form (m) of the precursors was monitored with respect to time. The amount of imported mature protein was detected by anti-DHFR antibody, quantified by densitometry, and illustrated in the form of a line graph. The maximal import rate for untransfected mitochondria was set to 100%.

Loss of respiratory complex activities leading to mitochondrial dysfunction often associates with the generation of reactive oxygen species (ROS) due to improper electron channeling, leading to the formation of superoxide and hydroxyl radicals. Therefore, to assess the effect of translocase B and translocase A downregulation in maintenance of free radical balance within the cell, HEK293T-silenced cells were stained for MitoSOX and DCFDA dye to adjudge the mitochondrial superoxide and total cellular peroxide levels, respectively. The absence of translocase B components leads to a significant elevation of the mitochondrial superoxide
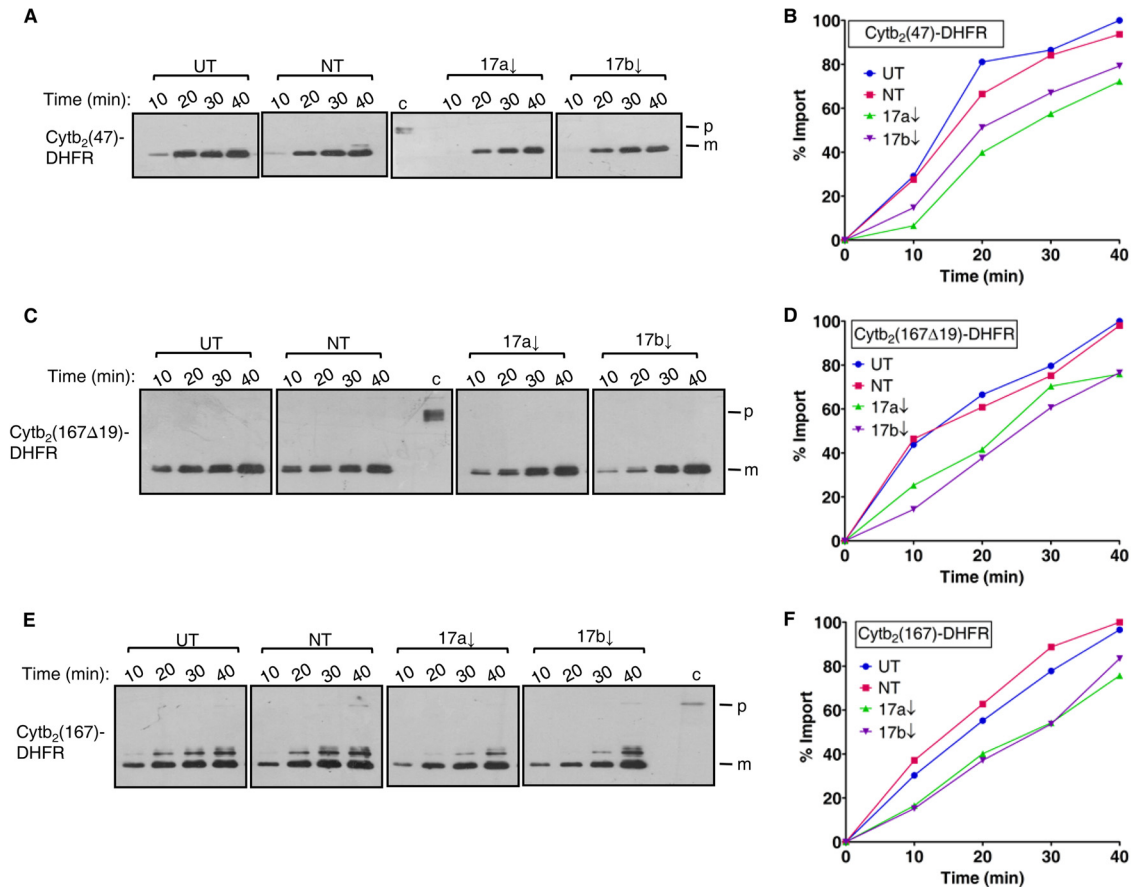
FIG 6 Rate of preprotein import by presequence translocases in cancer-derived LNCaP cells. To assess the effect of remodeled translocase organization on the protein import activity of translocases A and B, mitochondria isolated from LNCaP cells were subjected to comparative import assay as described for Fig. 5. The amount of imported mature protein (m) was quantified by densitometry and illustrated in form of a line graph. The maximum import rate for untransfected mitochondria was set to 100%.

levels (Fig. 9A), suggesting an inherent organellar defect, which in turn contributed to an increase in overall cellular ROS levels (Fig. 9B). In contrast, JC15 and Tim17a cells showed a slight increase in mitochondrial superoxide and cellular ROS (Fig. 9A and B). This highlights the critical role of translocase B in free radical metabolism in the organelle and that translocase A is not completely dispensable for mitochondrial homeostasis.

Finally, we assessed the effect of loss of respiration function on the morphology of mitochondria by fluorescence imaging using mtDsRed labeling. The control cells displayed small tube-shaped mitochondria (Fig. 9C). However, downregulation of Magmas, JC19, and Tim17b resulted in fragmentation, together with circular organellar morphology and reduction in mitochondrial density (Fig. 9C). On the contrary, depletion of JC15 and Tim17a leads to branching, elongation, and fusion of individual tubular mitochondria (Fig. 9C). This suggests that translocase A is not completely indispensable for mitochondrial integrity and underscores our previous observations on the essentiality of translocase B for maintenance of mitochondrial activity.

Loss of mitochondrial integrity and ATP drought coupled with prolonged levels of higher ROS cause the cells to accumulate mitochondrial DNA mutations, leading to its degradation and subsequent loss. Therefore, we assessed the maintenance of the mitochondrial genome (mtDNA) under the high-oxidative environment of knockdown cells by PCR amplifying the NADH dehydrogenase subunit I (ND1) and cytochrome oxidase subunit II (CO2) subunits. As expected, knockdown of translocase B components exhibits complete loss of mtDNA (Fig. 9D). Downregulation of translocase A, however, did not influence any detectable change in mtDNA levels (Fig. 9D). In summary, our data highlight the critical role of translocase B in the mitochondrial protein biogenesis, maintenance of ATP levels, redox balance, organellar morphology, and mtDNA integrity. Our finding also addresses the point that, though translocase A is nonessential for cell survival and basal import process, it plays a principal supportive role in governing proper mitochondrial function, as suggested by partial loss of mitochondrial activity and alteration in its morphology. It is therefore envisioned that translocase A might have additionally evolved a specialized role in the import of a subset of proteins that modulate mitochondrial functions, and the abolishment of the mitochondrial import of such proteins might be leading to fractional loss of organellar function.

Specific role of translocase A in human mitochondria. The translocase A component Tim17a had been previously documented to be overexpressed in clinical cases of breast cancer (22). Consistent with the idea of overexpressed translocase A components in cancer cells, our previous results demonstrate elevated levels of Tim17a and other translocase A components in prostate
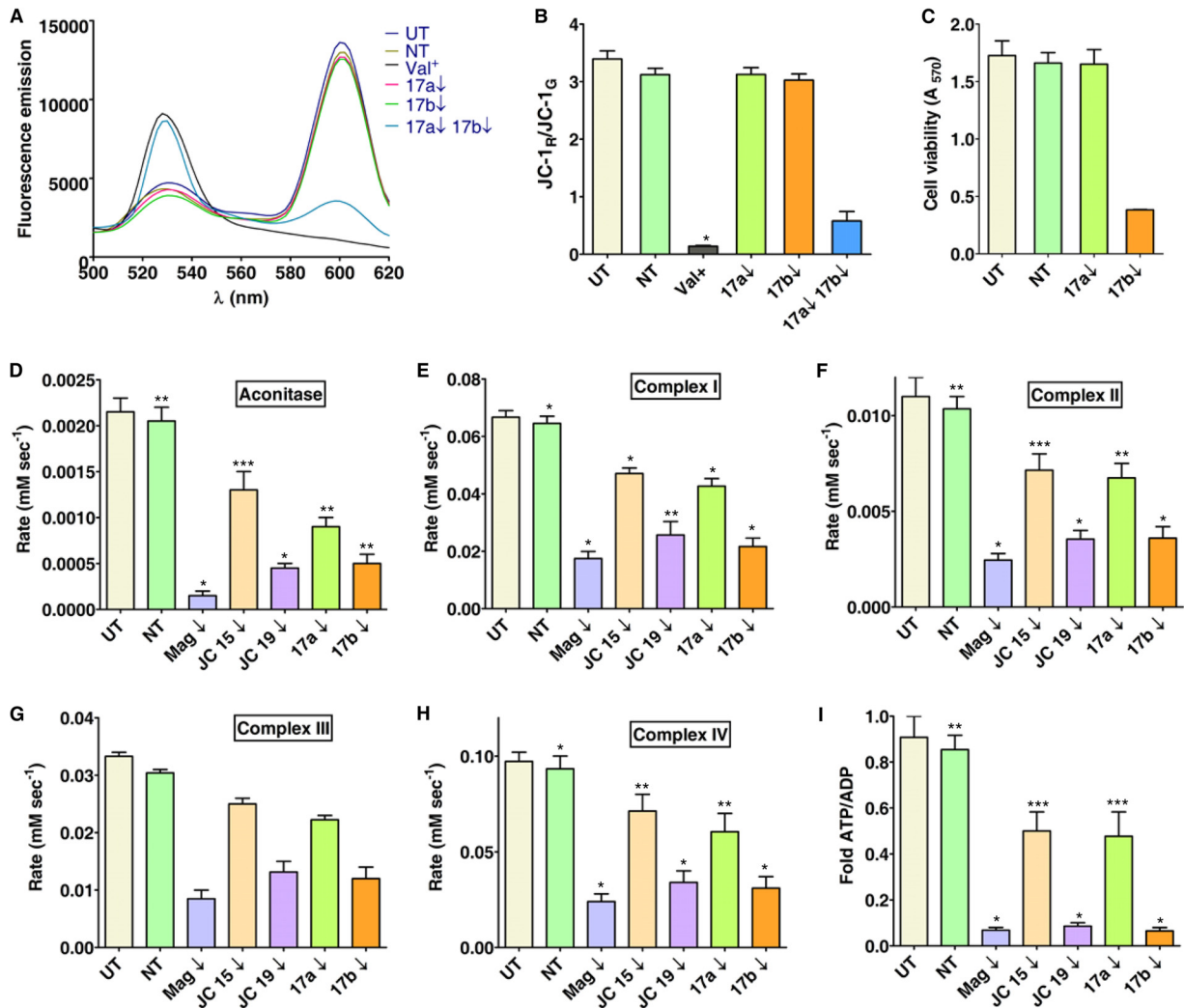
FIG 7 Comparative assessment of protein translocases in maintenance of mitochondrial function. (A and B) Loss of membrane potential upon Tim17 depletion. Mitochondria depleted for Tim17a, Tim17b, or both were stained with JC-1 and subjected to emission scan from 500 nm and 620 nm. The ratio of JC-1 red versus green fluorescence ($\lambda_{590}/\lambda_{530}$) was calculated and plotted on the bar chart (B), $n = 3$ experiments; P (two-tailed) < 0.001 unless otherwise indicated; *, P (two-tailed) < 0.0001. (C) HEK293T cells were transfected with siRNA pools against Tim17b and Tim17a. Forty-eight hours posttransfection, relative cell viability was measured using MTT assay, and data were represented as means ± standard errors of the means (SEM), $n = 8$ experiments; P (two-tailed) < 0.0001. (D) Effect of translocase activities on the mitochondria protein biogenesis was measured through aconitase activity by analyzing the rate of conversion of citrate to isocitrate and represented as means ± SEM, $n = 3$ experiments; *, P (two-tailed) < 0.0001; **, P (two-tailed) < 0.001; ***, P (two-tailed) < 0.01. (E to H) The electron transport chain function upon depletion of J-proteins alone or translocation complexes was addressed by evaluating the activities of individual complexes in isolated mitochondria. The specificity of the rate obtained for distinctive complexes was verified by inhibiting the corresponding complex by a specific inhibitor. Data plotted as means ± SEM, $n = 3$ experiments; *, P (two-tailed) < 0.0001; **, P (two-tailed) < 0.001; ***, P (two-tailed) < 0.01. (I) Fold alterations in mitochondrial ATP/ADP levels under J-proteins or translocase-deleted conditions are indicated as means ± SEM, $n = 3$ experiments; *, P (two-tailed) < 0.0001; **, P (two-tailed) < 0.001; ***, P (two-tailed) < 0.01. The ATP/ADP level in case of untransfected mitochondria was set to 1. All statistical analysis was performed using UT as the reference.

cancer cell lines (Fig. 3B). Indeed, assessment of the expression patterns in cancer cells from different origins presented higher levels of Tim17a and unaltered Tim17b amounts compared to those of noncancerous-origin HEK293T control cells (Fig. 10A). Initial studies in yeast have shown that overexpression of Tim17 prevents loss of mtDNA (34). Based on this information, we hypothesized that translocase A might be responsible for maintenance of copy number variation of the mitochondrial genome. We assessed the mtDNA levels in cells overexpressing Tim17a by two methods: first, by quantitative real-time PCR (qPCR) of two nucleotide segments from the regions in mtDNA, namely, ND1

and CO2, and second, by staining the isolated mitochondria from control or Tim17a-depleted cells with Sybr green dye, which fluoresces upon DNA binding. We observed that downregulation of Tim17a expression in HEK293T cells does not result in substantial alterations in the mtDNA copy numbers (Fig. 10B and D), and only a slight reduction was observed for Tim17a-depleted cells. In contrast, in cancer cell lines, we found that depletion of Tim17a caused a significant reduction in the mtDNA copy number at least by 5- to 7-fold, indicating a direct role of Tim17a in regulating an organellar DNA copy number in cancer cells (Fig. 10C, E, and F). These findings were further verified in different cancer-derived
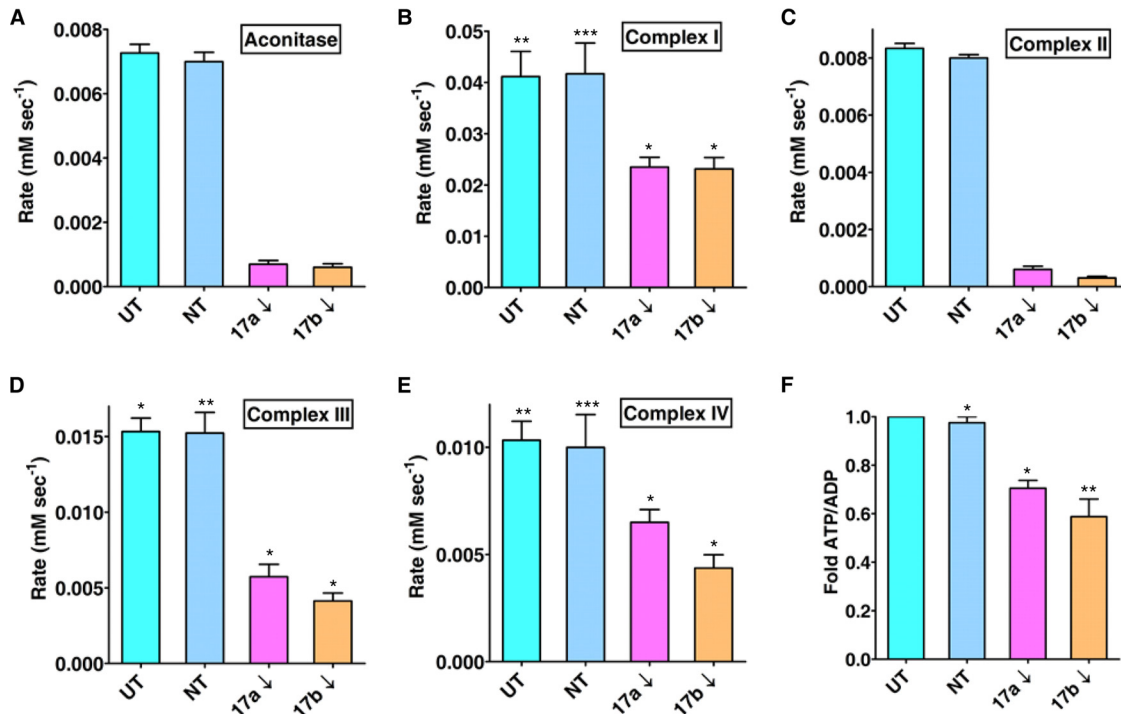
FIG 8 Role of translocases A and B in maintenance of mitochondrial activity in LNCaP cells. The importance of translocases A and B on mitochondrial protein biogenesis and sustenance of respiratory function was assessed as described for Fig. 7. Data are indicated as means ± SEM, $n = 3$ experiments; *, P (two-tailed) < 0.0001; **, P (two-tailed) < 0.001; ***, P (two-tailed) < 0.01. All statistical analysis was performed using UT as the reference.

cell lines from distinct origins, and similar results were observed (data not shown), indicating that elevated Tim17a levels in cancer cells maintain higher mtDNA copy numbers found in cancer cells.

Since higher mitochondrial DNA copy numbers are usually associated with uncontrollably proliferating cells, we tested whether Tim17a downregulation affected the proliferative potential of cells. In HEK293T cells, downregulation of Tim17a did not have any significant effect on the colony-forming ability of the cells, and the size of the colony formed was slightly smaller than the controls (Fig. 11A). In contrast, depletion of Tim17a in cancer-derived cells resulted in the inability of the cells to form larger colonies (Fig. 11B and C) than those of the controls and was found to be associated with increased generation time of cells (Fig. 11D and E). Indeed, Tim17a-depleted cells also showed lower DNA replicative potential than the controls, signifying reduced proliferative rates (Fig. 11F). To obtain a direct correlation between Tim17a overexpression and cell proliferation, we exogenously overexpressed Tim17a in HEK293T cells (Fig. 11G) and monitored the cellular proliferative rates. We observed that cells containing elevated amounts of Tim17a formed larger colonies, had shorter generation times, and showed increased incorporation of [^{3}H]thymidine compared to that of untransfected controls (Fig. 11H to J). In summary, our results propose that increased expression of translocase A enhances the proliferative potential of the cancer cells.

Previous reports have shown that mitochondrial distribution of certain cell signaling molecules maintains optimum levels of ETC complex function, leading to increased cell proliferation (21–23). Our data suggest that depletion of Tim17a causes partial ab-

rogation of ETC complex activity and, hence, mitochondrial function. Therefore, we hypothesized that translocase A might be particularly involved in mitochondrial translocation of specific noncanonical substrates that alter organellar function, leading to uncontrolled cell growth. Based on previous studies, we chose three substrates, namely, p53, Erk2, and STAT6, which are reported to localize in mitochondria in cancer cells as well as in cardiomyocytes, skeletal muscles, neuronal cells, and hematopoietic stem cells (24–26, 31–33, 35, 36). Expression of green fluorescent protein (GFP)-tagged constructs of p53, Erk2, and STAT6 in unsilenced MCF7 or LNCaP (data not shown) cells resulted in partitioning of these proteins into mitochondria (Fig. 12A to C). At the same time, depletion of translocase A abrogated the distribution of these proteins into mitochondria and resulted in their diffusion into the cytosol and nucleus (Fig. 12A to C). A similar result was observed in the case of subcellular fractionation in MCF7 cells. Immunodecoration with p53 or Erk2 antibodies indicated the presence of these proteins into the mitochondrial fraction (Fig. 12D and E, left). However, in the case of Tim17a depletion, bands corresponding to p53 or Erk2 were undetected in the mitochondrial fraction compared to in the controls, although the levels of these proteins in the cytosolic or nuclear fraction remained unaltered (Fig. 12D and E, left). Further, we detected specific bands similar to the phosphorylated forms of p53 and Erk2, indicating the localization of such active forms of these proteins into the organelle (Fig. 12D and E, left). In contrast, as a control, depletion of Tim17b, resulting in disruption of translocase B function, did not affect the localization of the p53 and Erk2 into the mitochondria (Fig. 12D and E, right). This shows that translocase
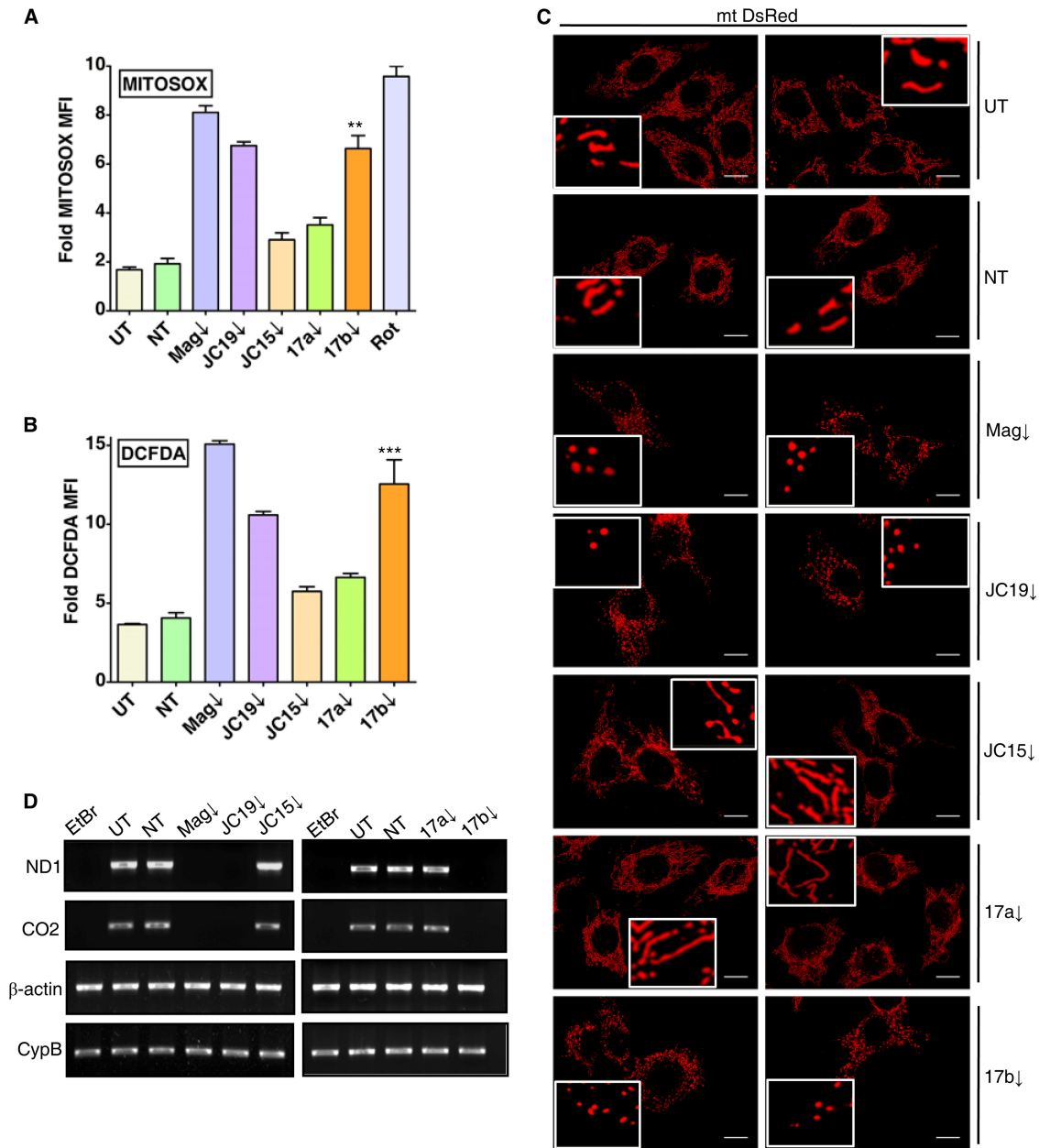
FIG 9 Loss of translocase function leads to organellar defects. (A and B) The effect of J-protein and translocase downregulation on mitochondrial superoxide levels (A) or overall cellular ROS balance (B) was measured by MitoSOX or DCFDA staining, respectively. The relative fluorescence intensity is represented as the fold mean florescence intensity (MFI) over unstained cells. Rotenone-treated cells (Rot) were used as a positive control for superoxide levels. Data denotes means $\pm$ SEM, $n = 3$ experiments; *, P (two-tailed) < 0.0001; **, P (two-tailed) < 0.001; ***, P (two-tailed) < 0.01. All statistical analysis was performed using UT as the reference. (C) Alterations in mitochondrial morphology were assessed by fluorescence imaging of mtDsRed-expressing HeLa cells depleted for J-proteins or Tim17 paralogs. Digitally zoomed images of isolated mitochondria are shown as an inset. (D) Mitochondrial DNA maintenance upon J-protein knockdown or depletion of either of the translocases was analyzed through amplification efficiency of mitochondrial genome open reading frames (ORFs), ND1 and CO2.

A has a specific function in translocation of these proteins into the mitochondria.

DISCUSSION

In the mammalian system, trafficking proteins involving a series of receptors, import pores, and diverse molecular machines into the organelle requires highly evolved and complex import machinery (21, 22). In contrast to yeast, human prese-

quence translocases exist in multiple numbers to accommodate the diverse repertoire of mitochondrion-targeted proteins. Mammalian translocases have diversified principally based on the presence of Tim17 and J-protein paralogs as constituting subunits and contain Tim50, Tim23, Tim44, and Magmas as the common channel components. The Tim17b isoforms together with JC19 form the mammalian-specific translocases B1 and B2 for robust constitutive mitochondrial functions. On the
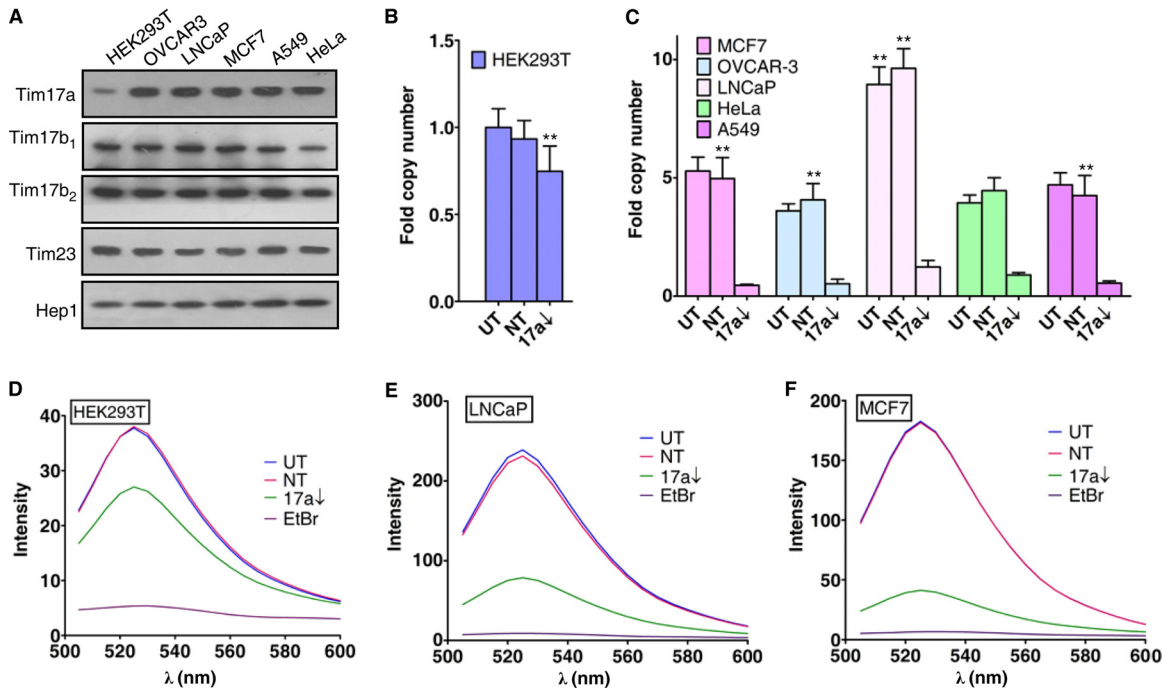
FIG 10 Involvement of translocase A in mitochondrial DNA copy number variation in cancer cells. (A) Relative expression of Tim17 paralogs in various cancer cell lines was analyzed by loading equivalent amounts of mitochondria followed by immunoblotting. (B and C) qPCR analysis of the mitochondrial genome of the indicated cell lines under untransfected or Tim17a-downregulated conditions normalized over genomic DNA controls. Bars represent means $\pm$ SEM, $n =$ 6 experiments; *, P (two-tailed) < 0.0001; **, P (two-tailed) < 0.001. All statistical analysis was performed using UT as the reference. (D to F) Representative lambda scan plots of three independent experiments depicting an amount of mitochondrial DNA for an equivalent amount of mitochondria, as a measure of bound Sybr green dye fluorescence.

contrary, translocase A having a Tim17a paralog partnered with JC15 forms the ancestral third translocase, which is non-essential for normal cell growth (Fig. 13). Indeed, translocase A showed an inability to import mitochondrial substrates as robustly as translocase B. Hence, we propose that the specificity of translocase function is governed mainly by Tim17 paralogs in association with particular J-proteins.

Magmas-like proteins have been previously implicated in tethering the J-proteins to the translocation channel (16, 17). Our results indicate that Magmas, in addition to its conserved function at human presequence translocase, regulates the distribution of individual J-proteins associated with the complex and thereby activates the translocases for neoplastic transformation under overexpressed conditions. In agreement with the idea, intrinsic overexpression of Magmas in prostate cancer and pituitary adenomas remodels the J-protein distribution at the TIM23 complex. A similar phenotype was observed upon exogenous elevation of Magmas protein levels that lead to redistribution and recruitment of J-proteins to either of the translocases, suggesting that Magmas plays a critical role in governing translocase activity. Indeed, reorganization of J-proteins at the import channel results in equivalent translocation activity for both translocases, and they play a synergistic role in the import of precursors into the mitochondria. The recruitment of JC19 to the primitive translocase A might aid in the import of several oncogenic proteins, tumor suppressors, and multidrug transporters, which are known to get translocated through unknown mechanisms in the cancer cells (23–25). On the other hand, depletion of JC19 from the essential translocases B1 and B2 may directly affect the import of preproteins, thus assisting the reprogramming of mitochondrial functions during cancer progression (26).

Under normal conditions, translocase B performs the essential function in maintenance of the overall import activity across the inner membrane, as indicated by its higher activity in terms of import kinetics for different mitochondrial substrates in comparison to translocase A. The rate of translocation of the precursor protein across translocase B was measured under translocase A-depleted conditions, whereas the import activity exhibited by translocase A was investigated by disruption of translocases B1 and B2. Optimum activity of translocase B is critical for normal mitochondrion function. Previous studies have shown an association of translocase component Tim21 with the electron transport chain machineries (20). Loss of translocase B leads to disruption in activities of the individual complexes of the respiratory chain, resulting in lower ATP and higher ROS levels caused by impaired electron channeling. Translocase B-depleted cells also showed reduced biogenesis of mitochondria and defective remodeling of the organelle with altered morphology. On the contrary, depletion of translocase A caused partial loss of respiratory complex activity and ATP levels and less-than-significant changes in the mitochondrial content, suggesting that it might play a role in import-specific molecules critical for mitochondrial respiration. However, in cancer cells, translocase A by virtue of its overexpression was found to play a comparable role in maintenance of organellar function. Depletion of either translocase A or B results in equivalent reductions in mitochondrial protein biogenesis and respiratory function.

Several components of translocase A, such as Tim17a, Magmas, and JC15, have been shown to be variably expressed in the subset of cancer cells (18, 31–33, 35, 36). Our previous experiments through CoIP analysis have shown specific overexpression of translocase A components in cancer-derived cell lines. How-
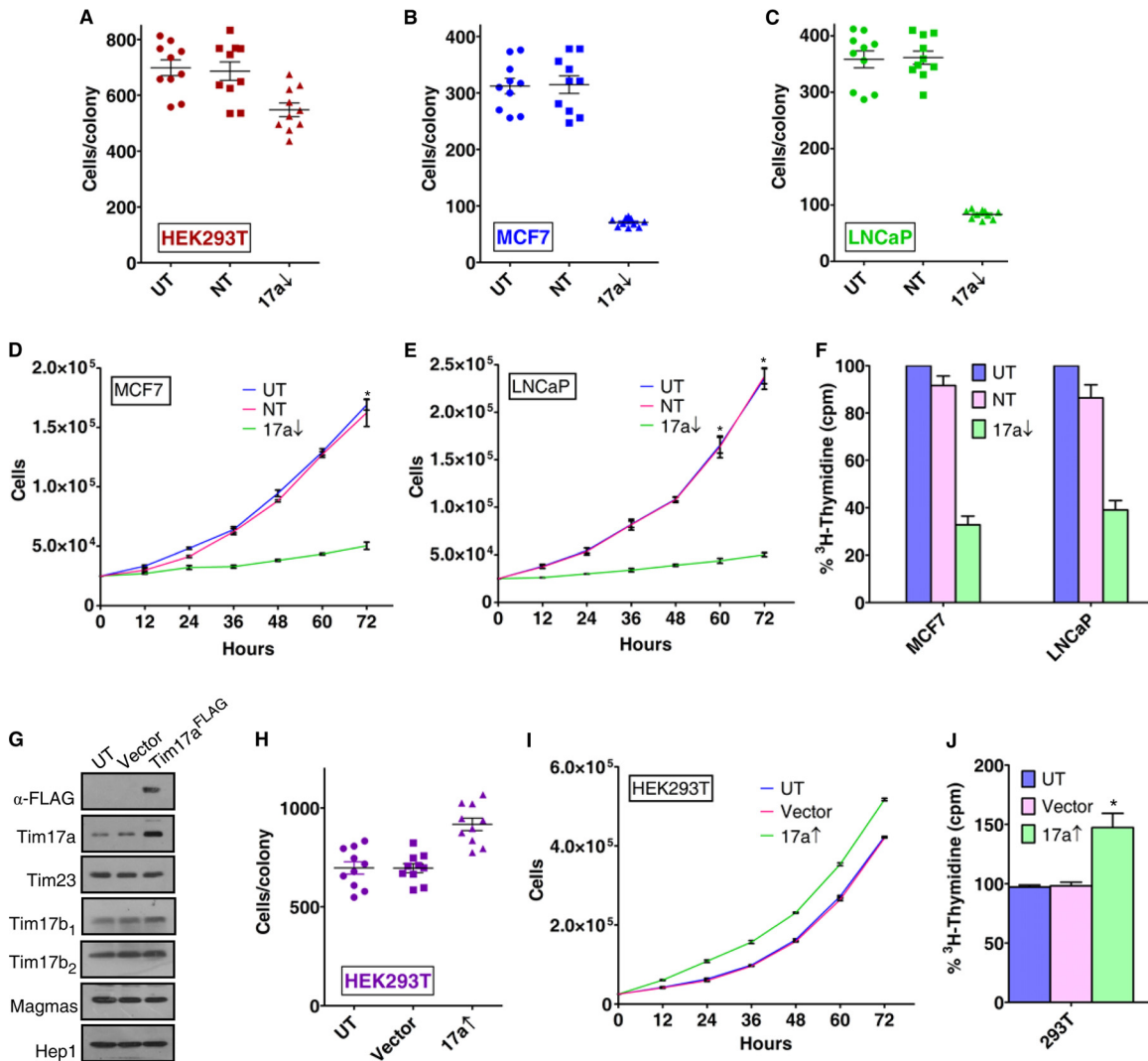
FIG 11 Association of translocase A with cellular proliferative rates. (A to C) Proliferative potential of cells under the Tim17a-knockdown condition was evaluated by counting the number of cells per isolated colony generated from a single-seeded cell over a period of 12 days. Data are represented as means ± SEM from 10 colonies accounted over three independent experiments. $P < 0.001$. (D and E) The effect of Tim17a downregulation on the generation time of the cells was analyzed by counting the cells at the indicated time periods and represented as means ± SEM, $n = 3$ experiments; P (two-tailed) < 0.001 unless otherwise indicated; *, P (two-tailed) < 0.01. (F) The proliferative potential of cancerous-origin MCF7 and LNCaP cells at the level of DNA replication was analyzed by growing equal numbers of cells in a pulse of [^{3}H]thymidine, and the amount of incorporated radioactivity was determined as counts per minute (cpm) and directly correlated with the rate of cell division. Bars represent means ± SEM, $n = 3$ experiments; P (two-tailed) < 0.001. (G) Immunoblot analysis of protein expression in mitochondria isolated from HEK293T cells transfected with a construct overexpressing Tim17a. (H to J) Colony-forming ability, generation time, and rate of DNA replication of Tim17a-overexpressing HEK293T (293T) cells were monitored as described earlier, to assess the proliferative potential of the cells. Data of all three experiments are represented as means ± SEM; P (two-tailed) < 0.001 unless otherwise indicated; *, P (two-tailed) < 0.01. All statistical analysis was performed using UT as the reference.

ever, the physiological significance of such as overexpression remained unresolved. The cancer cells have been known to accumulate higher copy numbers of the mtDNA. Several cellular oncoproteins localize into the cancer cell mitochondria, where they reprogram organellar functions, resulting in enhanced mitochondrial activity and unregulated proliferative potential within the cells that are hallmarks of cancer phenotypes. The translocase responsible for mitochondrial targeting of these proteins lacking the signal presequence is still not identified. Here, we provide first-time evidence in favor of a specific function of translocase A in the maintenance of a higher mtDNA copy number and translocation of substrates lacking a mitochondrion-targeting sequence (MTS). Previous reports have shown p53 to form a com-

plex with mitochondrial DNA where it is involved in a positive interaction with mitochondrial transcription factor A (TFAM) (34, 37). TFAM plays an important role in the maintenance and regulation of mtDNA content (38, 39). It is conceivable that translocase A-mediated accumulation of p53 in mitochondria might be enhancing TFAM activity, thereby elevating an mtDNA copy number in cancer cells. On the other hand, it is reasonable to believe that the lower basal import activity associated with translocase A may be critical for its unique function in importing non-MTS protein, which is known to depend on the translocation of other canonical mitochondrion-targeted proteins. Mitochondrial localization of substrates, such as the STAT family of proteins, is known to modulate the respiratory activities (40, 41), and preven-
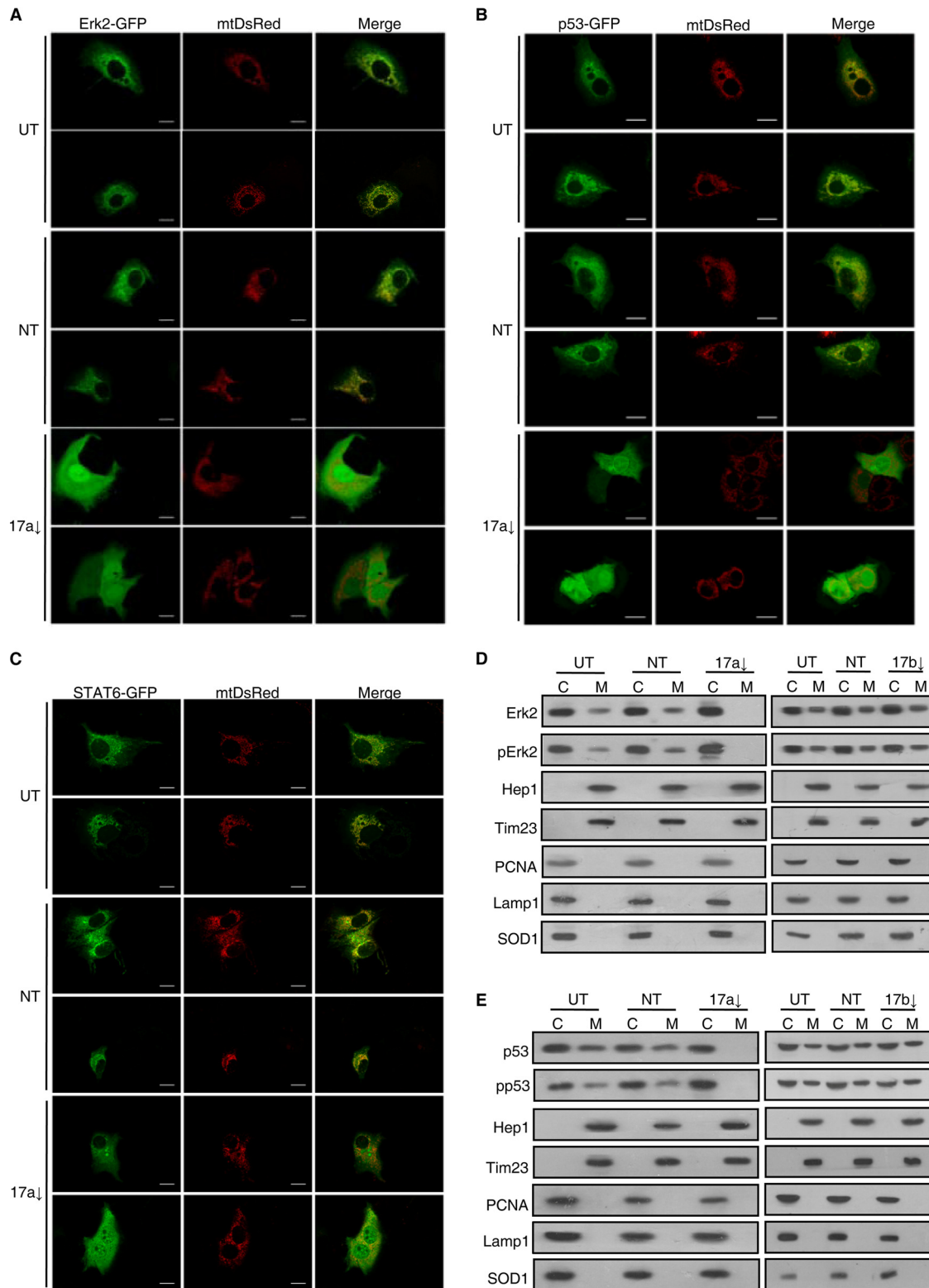
FIG 12 Role of translocase A in mitochondrial localization of proteins lacking mitochondrion-targeting presequence. (A to C) *In vivo* fluorescence imaging for subcellular distribution of GFP-tagged Erk2, p53, and STAT6 cotransfected with mtDsRed in MCF7 cells kept untransfected or depleted for translocase A. Red fluorescence denotes mtDsRed-labeled mitochondria. Green fluorescence shows subcellular distribution of the indicated protein. (D and E) Equivalent amounts of cytosolic nuclear extract (C) and a mitochondrial lysate (M) from untransfected and translocase A knockdown cells were immunoblotted using anti-p53- or anti-Erk2-specific antibodies along with other control antibodies as indicated. Translocase B-depleted cells were used as the internal control. Hep1 and Tim23 probing was done as mitochondrial marker proteins, PCNA was used as a nuclear marker, Lamp1 was used as an endosomal marker, and SOD1 was used as a cytosolic marker.
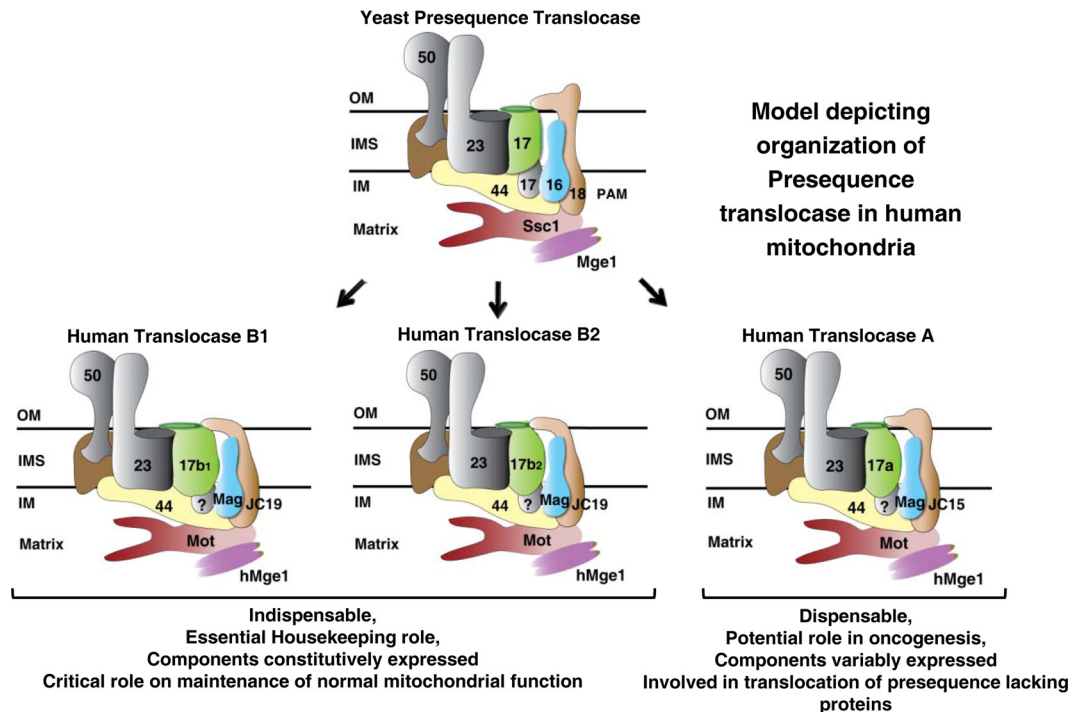
FIG 13 Schematic model depicting an organization of presequence translocase in human mitochondria. Translocase A containing DnaJC15 denotes the nonessential ancestral translocase with potential oncogenic functions. Translocases B1 and B2 constituting DnaJC19 are human-specific translocases carrying out essential housekeeping functions.

tion of mitochondrial distribution of these proteins results in reduced mitochondrial respiration, thus justifying the partial loss of ETC complex function in the case of Tim17a knockdown. However, the mitochondrial localization of these nuclear transcription factors is not limited in cancer cells and has been observed in skeletal muscles, cardiomyocytes, and neuronal cells, where they are known to modulate transcription of mitochondrial genes, ETC complexes, mitochondrial DNA copy number, and apoptotic pathways (42). Overall, we propose that translocase B performs the essential housekeeping function, whereas translocase A is specifically associated with processes involving cellular growth and division.

In summary, the present study delineates for the first time the intricate organization of human inner membrane presequence translocase machinery and the central role played by J-proteins for constitutive mitochondrial function and neoplastic transformation. Our study provides additional information for association of presequence translocase components in regulation of inner membrane complexes, such as an electron transport chain (43, 44), energy levels, and free radical balance in the cell. It also provides a line of evidence for a specific oncogenic role of nonessential translocase A, which could be utilized in the development of new strategies for cancer therapy. Further, the current work highlights a functional connection between regulation of mitochondrial DNA copy number and organellar partitioning of nodal signaling molecules by human presequence translocase A. However, the alterations in the signaling pathways mediated by translocase A leading to differential cell growth are still an open question for future investigation.

REFERENCES

1. **Neupert W, Herrmann JM.** 2007. Translocation of proteins into mitochondria. Annu. Rev. Biochem. **76:**723–749. http://dx.doi.org/10.1146/annurev.biochem.76.052705.163409.
2. **Chacinska A, Koehler CM, Milenkovic D, Lithgow T, Pfanner N.** 2009. Importing mitochondrial proteins: machineries and mechanisms. Cell **138:**628–644. http://dx.doi.org/10.1016/j.cell.2009.08.005.
3. **Kiebler M, Pfaller R, Sollner T, Griffiths G, Horstmann H, Pfanner N, Neupert W.** 1990. Identification of a mitochondrial receptor complex required for recognition and membrane insertion of precursor proteins. Nature **348:**610–616. http://dx.doi.org/10.1038/348610a0.
4. **Rehling P, Brandner K, Pfanner N.** 2004. Mitochondrial import and the twin-pore translocase. Nat. Rev. Mol. Cell. Biol. **5:**519–530. http://dx.doi.org/10.1038/nrm1426.
5. **Truscott KN, Voos W, Frazier AE, Lind M, Li Y, Geissler A, Dudek J, Muller H, Sickmann A, Meyer HE, Meisinger C, Guiard B, Rehling P, Pfanner N.** 2003. A J-protein is an essential subunit of the presequence translocase-associated protein import motor of mitochondria. J. Cell Biol. **163:**707–713. http://dx.doi.org/10.1083/jcb.200308004.
6. **Kozany C, Mokranjac D, Sichting M, Neupert W, Hell K.** 2004. The J domain-related cochaperone Tim16 is a constituent of the mitochondrial TIM23 preprotein translocase. Nat. Struct. Mol. Biol. **11:**234–241. http://dx.doi.org/10.1038/nsmb734.

7. Frazier AE, Dudek J, Guiard B, Voos W, Li Y, Lind M, Meisinger C, Geissler A, Sickmann A, Meyer HE, Bilanchone V, Cumsky MG, Truscott KN, Pfanner N, Rehling P. 2004. Pam16 has an essential role in the mitochondrial protein import motor. Nat. Struct. Mol. Biol. 11:226–233. http://dx.doi.org/10.1038/nsmb735.

8. Mokranjac D, Sichting M, Neupert W, Hell K. 2003. Tim14, a novel key component of the import motor of the TIM23 protein translocase of mitochondria. EMBO J. 22:4945–4956. http://dx.doi.org/10.1093/emboj/cdg485.

9. D'Silva PR, Schilke B, Walter W, Craig EA. 2005. Role of Pam16's degenerate J domain in protein import across the mitochondrial inner membrane. Proc. Natl. Acad. Sci. U. S. A. 102:12419–12424. http://dx.doi.org/10.1073/pnas.0505969102.

10. Tamura Y, Harada Y, Shiota T, Yamano K, Watanabe K, Yokota M, Yamamoto H, Sesaki H, Endo T. 2009. Tim23-Tim50 pair coordinates functions of translocators and motor proteins in mitochondrial protein import. J. Cell Biol. 184:129–141. http://dx.doi.org/10.1083/jcb.200808068.

11. Neupert W, Brunner M. 2002. The protein import motor of mitochondria. Nat. Rev. Mol. Cell. Biol. 3:555–565. http://dx.doi.org/10.1038/nrm878.

12. Liu Q, D'Silva P, Walter W, Marszalek J, Craig EA. 2003. Regulated cycling of mitochondrial Hsp70 at the protein import channel. Science 300:139–141. http://dx.doi.org/10.1126/science.1083379.

13. Pareek G, Samaddar M, D'Silva P. 2011. Primary sequence that determines the functional overlap between mitochondrial heat shock protein 70 Ssc1 and Ssc3 of Saccharomyces cerevisiae. J. Biol. Chem. 286:19001–19013. http://dx.doi.org/10.1074/jbc.M110.197434.

14. Tamura Y, Harada Y, Yamano K, Watanabe K, Ishikawa D, Ohshima C, Nishikawa S, Yamamoto H, Endo T. 2006. Identification of Tam41 maintaining integrity of the TIM23 protein translocator complex in mitochondria. J. Cell Biol. 174:631–637. http://dx.doi.org/10.1083/jcb.200603087.

15. Jensen RE, Dunn CD. 2002. Protein import into and across the mitochondrial inner membrane: role of the TIM23 and TIM22 translocons. Biochim. Biophys. Acta 1592:25–34. http://dx.doi.org/10.1016/S0167-4889(02)00261-6.

16. Sinha D, Joshi N, Chittoor B, Samji P, D'Silva P. 2010. Role of Magmas in protein transport and human mitochondria biogenesis. Hum. Mol. Genet. 19:1248–1262. http://dx.doi.org/10.1093/hmg/ddq002.

17. D'Silva PR, Schilke B, Hayashi M, Craig EA. 2008. Interaction of the J-protein heterodimer Pam18/Pam16 of the mitochondrial import motor with the translocon of the inner membrane. Mol. Biol. Cell 19:424–432. http://dx.doi.org/10.1091/mbc.E07-08-0748.

18. Jubinsky PT, Short MK, Mutema G, Morris RE, Ciraolo GM, Li M. 2005. Magmas expression in neoplastic human prostate. J. Mol. Histol. 36:69–75. http://dx.doi.org/10.1007/s10735-004-3840-8.

19. Tagliati F, Gentilin E, Buratto M, Mole D, degli Uberti EC, Zatelli MC. 2010. Magmas, a gene newly identified as overexpressed in human and mouse ACTH-secreting pituitary adenomas, protects pituitary cells from apoptotic stimuli. Endocrinology 151:4635–4642. http://dx.doi.org/10.1210/en.2010-0441.

20. Mick DU, Dennerlein S, Wiese H, Reinhold R, Pacheu-Grau D, Lorenzi I, Sasarman F, Weraarpachai W, Shoubridge EA, Warscheid B, Rehling P. 2012. MITRAC links mitochondrial protein translocation to respiratory-chain assembly and translational regulation. Cell 151:1528–1541. http://dx.doi.org/10.1016/j.cell.2012.11.053.

21. Bauer MF, Gempel K, Reichert AS, Rappold GA, Lichtner P, Gerbitz KD, Neupert W, Brunner M, Hofmann S. 1999. Genetic and structural characterization of the human mitochondrial inner membrane translocase. J. Mol. Biol. 289:69–82. http://dx.doi.org/10.1006/jmbi.1999.2751.

22. Sheng ZH, Cai Q. 2012. Mitochondrial transport in neurons: impact on synaptic homeostasis and neurodegeneration. Nat. Rev. Neurosci. 13:77–93. http://dx.doi.org/10.1038/nrg3141.

23. Costantini P, Jacotot E, Decaudin D, Kroemer G. 2000. Mitochondrion as a novel target of anticancer chemotherapy. J. Natl. Cancer Inst. 92:1042–1053. http://dx.doi.org/10.1093/jnci/92.13.1042.

24. Fulda S, Galluzzi L, Kroemer G. 2010. Targeting mitochondria for cancer therapy. Nat. Rev. Drug Discov. 9:447–464. http://dx.doi.org/10.1038/nrd3137.

25. Gogvadze V, Orrenius S, Zhivotovsky B. 2008. Mitochondria in cancer cells: what is so special about them? Trends Cell Biol. 18:165–173. http://dx.doi.org/10.1016/j.tcb.2008.01.006.

26. Kroemer G, Pouyssegur J. 2008. Tumor cell metabolism: cancer's Achilles' heel. Cancer Cell 13:472–482. http://dx.doi.org/10.1016/j.ccr.2008.05.005.

27. Schneider HC, Berthold J, Bauer MF, Dietmeier K, Guiard B, Brunner M, Neupert W. 1994. Mitochondrial Hsp70/MIM44 complex facilitates protein import. Nature 371:768–774. http://dx.doi.org/10.1038/371768a0.

28. D'Silva PD, Schilke B, Walter W, Andrew A, Craig EA. 2003. J protein cochaperone of the mitochondrial inner membrane required for protein import into the mitochondrial matrix. Proc. Natl. Acad. Sci. U. S. A. 100:13839–13844. http://dx.doi.org/10.1073/pnas.1936150100.

29. Livak KJ, Schmittgen TD. 2001. Analysis of relative gene expression data using real-time quantitative PCR and the 2(-Delta Delta C(T)) method. Methods 25:402–408. http://dx.doi.org/10.1006/meth.2001.1262.

30. Spinazzi M, Casarin A, Pertegato V, Salviati L, Angelini C. 2012. Assessment of mitochondrial respiratory chain enzymatic activities on tissues and cultured cells. Nat. Protoc. 7:1235–1246. http://dx.doi.org/10.1038/nprot.2012.058.

31. Salhab M, Patani N, Jiang W, Mokbel K. 2012. High TIMM17A expression is associated with adverse pathological and clinical outcomes in human breast cancer. Breast Cancer 19:153–160. http://dx.doi.org/10.1007/s12282-010-0228-3.

32. Shridhar V, Bible KC, Staub J, Avula R, Lee YK, Kalli K, Huang H, Hartmann LC, Kaufmann SH, Smith DI. 2001. Loss of expression of a new member of the DNAJ protein family confers resistance to chemotherapeutic agents used in the treatment of ovarian cancer. Cancer Res. 61:4258–4265.

33. Schusdziarra C, Blamowska M, Azem A, Hell K. 2013. Methylation-controlled J-protein MCJ acts in the import of proteins into human mitochondria. Hum. Mol. Genet. 22:1348–1357. http://dx.doi.org/10.1093/hmg/dds541.

34. Saleem A, Hood DA. 2013. Acute exercise induces tumour suppressor protein p53 translocation to the mitochondria and promotes a p53-Tfam-mitochondrial DNA complex in skeletal muscle. J. Physiol. 591:3625–3636. http://dx.doi.org/10.1113/jphysiol.2013.252791.

35. Lindsey JC, Lusher ME, Strathdee G, Brown R, Gilbertson RJ, Bailey S, Ellison DW, Clifford SC. 2006. Epigenetic inactivation of MCJ (DNAJD1) in malignant paediatric brain tumours. Int. J. Cancer 118:346–352. http://dx.doi.org/10.1002/ijc.21353.

36. Strathdee G, Vass JK, Oien KA, Siddiqui N, Curto-Garcia J, Brown R. 2005. Demethylation of the MCJ gene in stage III/IV epithelial ovarian cancer and response to chemotherapy. Gynecol. Oncol. 97:898–903. http://dx.doi.org/10.1016/j.ygyno.2005.03.023.

37. Park JY, Wang PY, Matsumoto T, Sung HJ, Ma W, Choi JW, Anderson SA, Leary SC, Balaban RS, Kang JG, Hwang PM. 2009. p53 improves aerobic exercise capacity and augments skeletal muscle mitochondrial DNA content. Circ. Res. 105:705–712. http://dx.doi.org/10.1161/CIRCRESAHA.109.205310.

38. Ekstrand MI, Falkenberg M, Rantanen A, Park CB, Gaspari M, Hultenby K, Rustin P, Gustafsson CM, Larsson NG. 2004. Mitochondrial transcription factor A regulates mtDNA copy number in mammals. Hum. Mol. Genet. 13:935–944. http://dx.doi.org/10.1093/hmg/ddh109.

39. Kaufman BA, Durisic N, Mativetsky JM, Costantino S, Hancock MA, Grutter P, Shoubridge EA. 2007. The mitochondrial transcription factor TFAM coordinates the assembly of multiple DNA molecules into nucleoid-like structures. Mol. Biol. Cell 18:3225–3236. http://dx.doi.org/10.1091/mbc.E07-05-0404.

40. Wegrzyn J, Potla R, Chwae YJ, Sepuri NB, Zhang Q, Koeck T, Derecka M, Szczepanek K, Szelag M, Gornicka A, Moh A, Moghaddas S, Chen Q, Bobbili S, Cichy J, Dulak J, Baker DP, Wolfman A, Stuehr D, Hassan MO, Fu XY, Avadhani N, Drake JI, Fawcett P, Lesnefsky EJ, Larner AC. 2009. Function of mitochondrial Stat3 in cellular respiration. Science 323:793–797. http://dx.doi.org/10.1126/science.1164551.

41. Matoba S, Kang JG, Patino WD, Wragg A, Boehm M, Gavrilova O, Hurley PJ, Bunz F, Hwang PM. 2006. p53 regulates mitochondrial respiration. Science 312:1650–1653. http://dx.doi.org/10.1126/science.1126863.

42. Szczepanek K, Lesnefsky EJ, Larner AC. 2012. Multi-tasking: nuclear transcription factors with novel roles in the mitochondria. Trends Cell Biol. 22:429–437. http://dx.doi.org/10.1016/j.tcb.2012.05.001.

43. Roy S, Short MK, Stanley ER, Jubinsky PT. 2012. Essential role of Drosophila black-pearl is mediated by its effects on mitochondrial respiration. FASEB J. 26:3822–3833. http://dx.doi.org/10.1096/fj.11-193540.

44. Wiedemann N, van der Laan M, Hutu DP, Rehling P, Pfanner N. 2007. Sorting switch of mitochondrial presequence translocase involves coupling of motor module to respiratory chain. J. Cell Biol. 179:1115–1122. http://dx.doi.org/10.1083/jcb.200709087.